Cell Stem Cell

Short article

Synthetic immune checkpoint engagers protect HLA-deficient iPSCs and derivatives from innate immune cell cytotoxicity

Graphical abstract

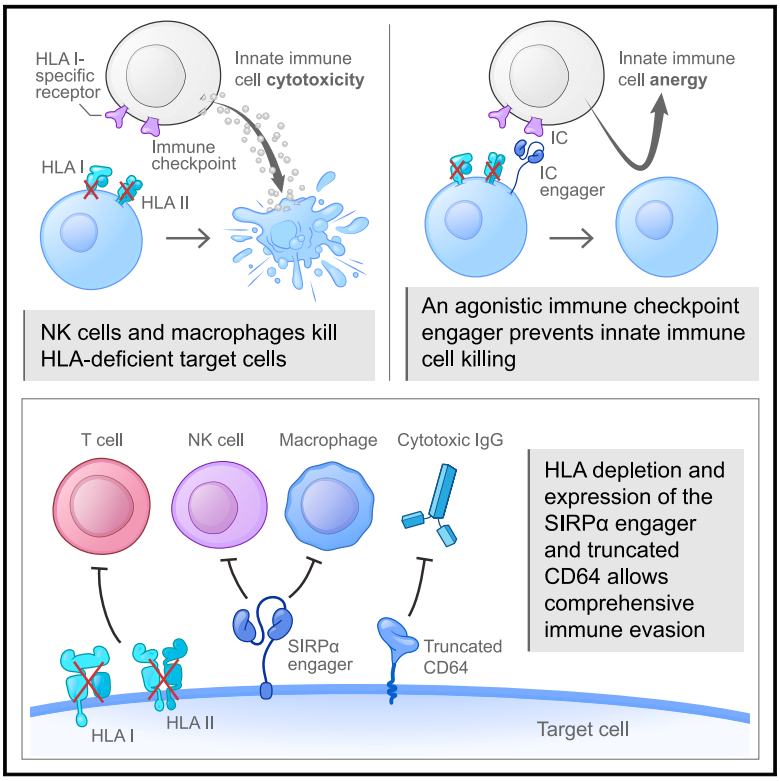

Highlights

- Synthetic cell surface molecules inhibit cytotoxicity by adjacent immune cells
- Different designs affect immune checkpoints in NK cells, macrophages, or T cells
- Engager molecules can exploit so-far-unused pathways for immune evasion
- The SIRPα engager synergizes with additional hypoimmune strategies

Authors

Alessia Gravina, Grigol Tediashvili, Yueting Zheng, ..., Mitsujiro Osawa, Sonja Schrepfer, Tobias Deuse

Correspondence

tobias.deuse@ucsf.edu

In brief

Deuse and colleagues design and test a new class of synthetic cell surface molecules that activates immune checkpoints in immune cells and inhibits cytotoxicity. These agonistic engager molecules target different immune cell populations and could help protect allogeneic immune-oncology or regenerative cell therapeutics from rejection and improve their efficacy.

Gravina et al., 2023, Cell Stem Cell *30*, 1538–1548
November 2, 2023
https://doi.org/10.1016/j.stem.2023.10.003

CellPress

CellPress
OPEN ACCESS

Cell Stem Cell

Short article

Synthetic immune checkpoint engagers protect HLA-deficient iPSCs and derivatives from innate immune cell cytotoxicity

Alessia Gravina,[1] Grigol Tediashvili,[1] Yueting Zheng,[2] Kumiko A. Iwabuchi,[2] Sara M. Peyrot,[2] Susan Z. Roodsari,[2] Lauren Gargiulo,[2] Shin Kaneko,[3] Mitsujiro Osawa,[4] Sonja Schrepfer,[1,5] and Tobias Deuse[1,5,6,*]

[1]Transplant and Stem Cell Immunobiology (TSI)-Lab, Department of Surgery, University of California, San Francisco, 513 Parnassus Avenue, San Francisco, CA 94143, USA

[2]Shinobi Therapeutics, 2 Tower Place, South San Francisco, CA 94080, USA

[3]Laboratory of Regenerative Immunotherapy, Department of Cell Growth and Differentiation, Center for iPS cell Research, Kyoto University, Sakyo-ku, Kyoto, Japan

[4]Shinobi Therapeutics, Med-Pharm Collaboration Building 46-29, Yoshida-Shimo-Adachi-Cho, Sakyo-Ku, Kyoto, Japan

[5]These authors contributed equally

[6]Lead contact

*Correspondence: tobias.deuse@ucsf.edu

https://doi.org/10.1016/j.stem.2023.10.003

SUMMARY

Immune rejection of allogeneic cell therapeutics remains a major problem for immuno-oncology and regenerative medicine. Allogeneic cell products so far have inferior persistence and efficacy when compared with autologous alternatives. Engineering of hypoimmune cells may greatly improve their therapeutic benefit. We present a new class of agonistic immune checkpoint engagers that protect human leukocyte antigen (HLA)-depleted induced pluripotent stem cell-derived endothelial cells (iECs) from innate immune cells. Engagers with agonistic functionality to their inhibitory receptors TIM3 and SIRPα effectively protect engineered iECs from natural killer (NK) cell and macrophage killing. The SIRPα engager can be combined with truncated CD64 to generate fully immune evasive iECs capable of escaping allogeneic cellular and immunoglobulin G (IgG) antibody-mediated rejection. Synthetic immune checkpoint engagers have high target specificity and lack retrograde signaling in the engineered cells. This modular design allows for the exploitation of more inhibitory immune pathways for immune evasion and could contribute to the advancement of allogeneic cell therapeutics.

INTRODUCTION

One of the most demanding challenges remaining for the field of regenerative medicine is the protection of allogeneic stem cell-derived therapeutics from immune rejection.[1] Hypoimmune induced pluripotent stem cell (iPSC)-derived pancreatic beta cells for the treatment of type 1 diabetes mellitus are currently being developed and initial proof of concept has been established.[2,3] Also, after initial success of autologous chimeric antigen receptor (CAR) T cells for the treatment of hematologic CD19$^+$ cancers, next-generation allogeneic immune therapeutics are currently being developed.[4–7] For regenerative and immune-oncology products, gene-engineered immune evasion could make cell therapeutics fully resistant to immune rejection, thus turning them into universal off-the-shelf products at lower cost for larger patient populations.

The development of iPSC differentiation protocols for cell therapeutics markedly facilitates large-scale manufacturing of well-defined and quality-controlled products. To prevent T cell-mediated allograft rejection, several groups have successfully depleted cells of human leukocyte antigen (HLA) class I and II molecules.[2,8–10] In line with the "missing self" theory, this strategy requires additional immune edits to silence innate immune cells, which naturally attack cells not expressing HLA class I. Innate immune cells have several inhibitory pathways that can be exploited to inhibit the killing of HLA class I-deficient cells. Overexpression of cognate ligands for such inhibitory receptors has been described for CD47,[8] HLA-E,[11] HLA-G,[12] and HLA-C.[13] Additionally, the knockout (KO) of PVR, a concomitantly expressed ligand for the activating receptor DNAM-1, was shown to contribute to reducing natural killer (NK) cell cytotoxicity.[9] However, the expression of full-size proteins may induce unwanted retrograde signaling in the engineered cells with perturbations of their physiology or may alter the differentiation potential of engineered iPSCs. Immune edits for the purpose of generating hypoimmune cells should ideally only have outward-facing immune inhibitory efficacy without retrograde intracellular signaling. Also, most natural ligands lack specificity for their inhibitory immune cell receptors and have additional binding partners or functions, which could obscure their net efficacy.

CellPress
OPEN ACCESS

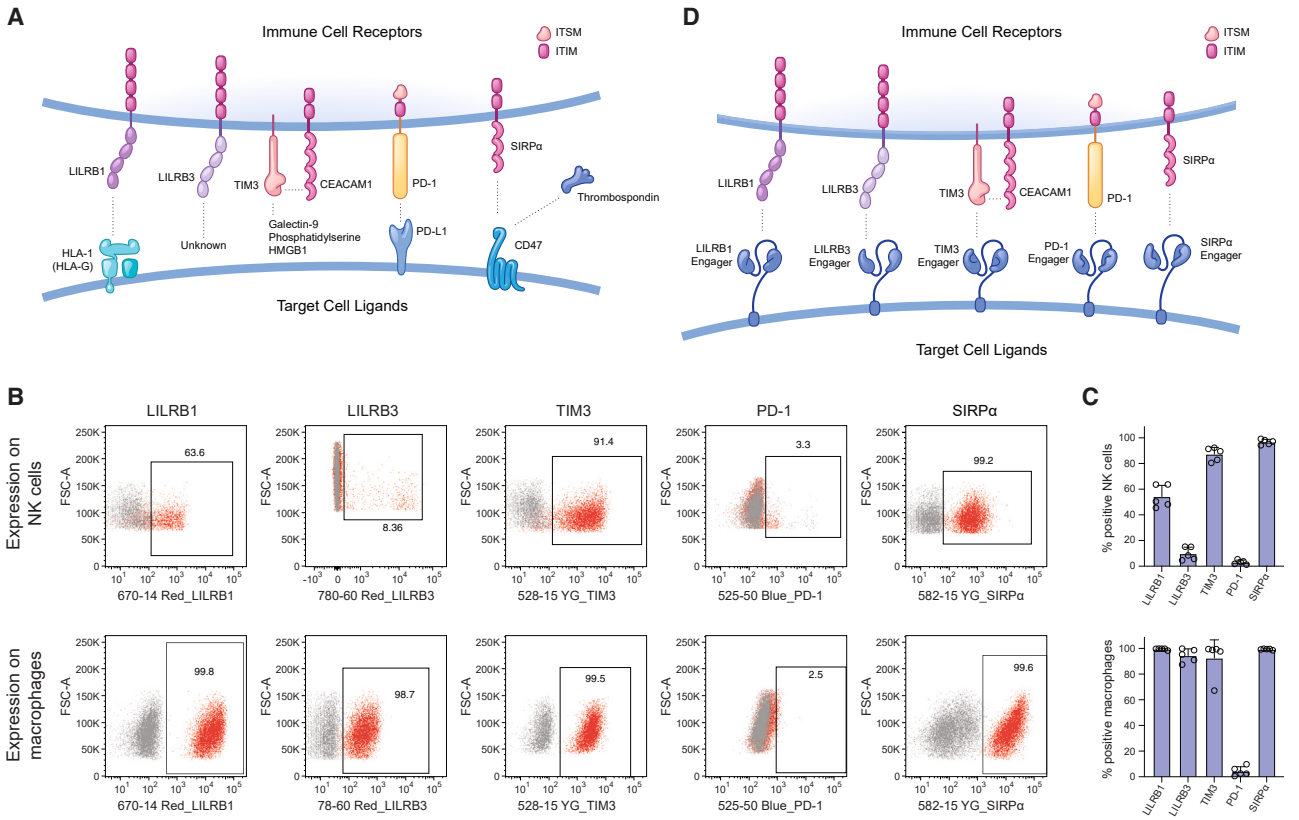

Figure 1. Synthetic immune cell checkpoint engagers

(A) The use of the immune cell receptors LILRB1, LILRB3, TIM3, PD-1, and SIRPα for the protection of cell therapeutics against innate immune cell killing comes with different challenges related to their natural ligands.

(B and C) The expression of LILRB1, LILRB3, TIM3, PD-1, and SIRPα on primary human NK cells and macrophages is shown (representative flow cytometry histograms, B; mean ± SD, n = 5, C). The percentage of positive cells is presented.

(D) Synthetic immune cell checkpoint engagers with agonistic function were designed for LILRB1, LILRB3, TIM3, PD-1, and SIRPα. All engagers have specific binding domains for the immune cell receptors, are membrane-bound, and lack intracellular domains.

Additional edits need to be added to protect cell therapeutics from cytotoxic immunoglobulin G (IgG) antibodies, and two different approaches have recently been presented.[14,15] We herein describe the engineering of a new class of highly specific synthetic immune cell checkpoint engagers and their use for the engineering of completely immune-protected cell therapeutics.

RESULTS

Designing synthetic immune cell checkpoint engagers

Inhibitory innate immune cell receptors include LILRB1, LILRB3, TIM3, PD-1, and SIRPα[16,17] (Figure 1A). LILRB1 is broadly expressed by myeloid cells and a subset of NK cells[18] and binds to HLA class I proteins, with the highest affinity for HLA-G.[19] On HLA class I and II KO (double KO [DKO]) hypoimmune cells, LILRB1 has no ligand, and this pathway remains unused for additional inhibitory immune signals. LILRB3 is restrictively expressed on myeloid cells, and like LILRB1, it belongs to the immunoreceptor tyrosine-based inhibitory motif (ITIM)-containing LILRB family.[20] Since no LILRB3 ligand has yet been identified, this pathway has not been used for hypoimmune editing. TIM3 is constitutively expressed by all mature NK cells and is also found on myeloid cells.[21] Although it has no characteristic inhibitory signaling motifs in its cytoplasmic domain, TIM3 has been shown to form heterodimers with CEACAM1, which contains conical ITIMs.[22] Numerous ligands have been proposed for TIM3, including galectin-9, phosphatidylserine, HMGB1, and CEACAM1, and although it is widely regarded as an inhibitory receptor, under some circumstances TIM3 may serve as an activating receptor.[23] Uncertainty around its ligands and their unresolved contrasting functional behaviors have so far prevented the utilization of the TIM3 pathway for immune editing. PD-1 has been extensively studied in T cells, and overexpression of its ligand PD-L1 on human islet-like organoid xenografts protected them from rejection in immune-competent diabetic mice.[24] However, PD-1 is not frequently expressed at relevant levels on NK cells,[2,25] and its use for inhibiting innate immune cells is questionable. CD47 is a complex molecule that binds to SIRPα in *cis* and *trans* interactions and has thrombospondin as additional binding partner. It further engages in lateral interactions with other signaling receptors, and several of these interactions are perturbed by ligand binding to CD47.[26] CD47 has been shown to be involved in Ca^{2+} signaling, cell adhesion, migration, and apoptosis.[27] A synthetic ligand for immune cell SIRPα lacking retrograde signaling only has outward function.

Human peripheral blood macrophages and interleukin (IL)-2-activated NK cells were assessed for their expression of those immune checkpoints (Figures 1B and 1C). TIM3 and SIRPα were expressed on the majority of both NK cells and macrophages, with SIRPα appearing to be the most robustly expressed checkpoint receptor. LILRB1 and LILRB3 showed high expression on all macrophages but were only expressed on a fraction of NK cells. PD-1 was expressed on a minority of NK cells and on no macrophages.

Synthetic immune cell checkpoint engagers were generated from highly specific antibodies against LILRB1, LILRB3, TIM3, PD-1, and SIRPα for which agonistic function had been described (Figure 1D). Antibody single-chain variable fragments (scFvs) were attached to the CD8α hinge sequence, the platelet-derived growth factor receptor (PDGFR) transmembrane domain, and lacked any intracellular domains to rule out retrograde signaling. The engager sequences were cloned into lentiviral particles that also included an RFP tag. *B2M*$^{-/-}$ *CIITA*$^{-/-}$ (DKO) iPSC-derived endothelial cells (iECs) were transduced with one of the 5 engager lentiviruses to generate DKO-engager pools. Fully edited DKO-engager cells were then sorted using the RFP tag.

Immune checkpoint engagers inhibit innate immune cells

First, the functionality of the engagers was assessed using highly sensitive *in vitro* impedance cytotoxicity assays with IL-2-activated NK cells or macrophages as effector cells in different effector-to-target cell ratios (E:T ratios). Target cells were DKO iECs and the 5 DKO-engager iECs. The target cells were plated on electrode plates, and the cell index was normalized at steady state. In this assay, any cytotoxicity that disturbs the target cell covering of the electrodes leads to a decrease of impedance, and the cell index drops. Target cells were also transduced to express firefly luciferase so that cytotoxicity could additionally be quantified through the drop of their ATP-dependent bioluminescence signals after the addition of effector cells. DKO iECs were killed increasingly rapidly with increasing E:T ratios of NK cell or macrophage effector cells (Figures 2A and S1A). The two engagers for TIM3 and SIRPα were both successful in fully protecting the HLA-depleted cells from innate killing (Figures 2B, 2C, S1B, and S1C). That correlated well with the high expression levels of their checkpoint receptors on both innate immune cell populations. LILRB1 and LILRB3, however, were only broadly expressed on macrophages but not on NK cells, and the DKO$^{LILRB1\text{-}E}$ and DKO$^{LILRB3\text{-}E}$ cells were only protected against macrophage killing (Figures S1D, S1E, S2A, and S2B). PD-1 was only expressed on a very small NK cell population but not on macrophages, and the PD-1 engager did not protect against either cell population (Figures S1F and S2C). However, the efficacy of the PD-1 engager could be demonstrated when only PD-1^{+} NK cells were sorted and used for the cytotoxicity assay (Figure S2D). In this case, DKO$^{PD\text{-}1\text{-}E}$ cells were protected even against high PD-1^{+} NK cell E:T ratios. Since PD-1 is an established immune checkpoint in T cells, we tested the activity of the PD-1 engager to protect HLA-A2-replete wild-type (WT) iECs against HLA-A2-reactive CD8 T cells (Figures S1G–S1K). While the WT iECs were killed in a T cell-typical kinetic, the WT$^{PD\text{-}1\text{-}E}$ cells were protected. CD47 has shown reliable efficacy against NK cell and macrophage killing in previous studies. We therefore generated DKO^{CD47} cells and confirmed their protection against innate immune killing (Figures S3A–S3C). Together, these results show that the two synthetic engagers for TIM3 and SIRPα were able to fully prevent innate immune killing induced by HLA deficiency.

Engagers bind immune cell checkpoints

The binding of the 2 engagers for TIM3 and SIRPα to their respective receptors was assessed. We found both selected engager molecules were highly expressed in the sorted DKO-engager populations (Figure S3D). To test the binding capacity of these synthetic engagers, we performed flow cytometry binding assays with recombinant SIRPα and TIM3 (Figure S3E). Both engager cells showed very good binding to their respective receptor proteins. Some minor binding of recombinant SIRPα to DKO could be attributed to their basal CD47 expression (Figure S3F). Next, we wanted to investigate whether certain expression threshold levels for the engagers were required to provide immune protection. DKO cells were transduced with one of the lentiviruses carrying the TIM3 engager or SIRPα engager and low-, medium-, and high-expressing subpopulations were sorted (Figures S4A and S4B). In bioluminescence imaging (BLI) killing assays, the low-expressing engager populations were killed, while the medium- and high-expressing populations were protected (Figures S4C and S4D). None of the engagers required very high expression levels that would be difficult to achieve in cell products. An antibody binding the G4S linker in the SIRPα engager construct was used next to evaluate surface expression and potential downregulation upon binding to SIRPα (Figures S4E–S4H). A small downregulation was observed when the DKO$^{SIRP\alpha\text{-}E}$ cells were incubated with human recombinant SIRPα protein or macrophages constitutively expressing SIRPα. Since incubation with cells expressing the immune checkpoints seemed more physiologic, we incubated DKO$^{LILRB1\text{-}E}$ cells with macrophages and DKO$^{TIM3\text{-}E}$ cells with NK cells, which constitutively express these receptors (Figures S4I–S4L). Overall, the downregulation of all engagers was very subtle considering the wide range of effective expression levels shown above. Since SIRPα seemed the most robust immune checkpoint in innate immune cells, we chose to further advance this engager. To confirm that direct binding of the SIRPα engager to its receptor SIRPα was mechanistically necessary for the observed protection from innate cell killing, we performed cytotoxicity assays with an abundance of free SIRPα protein that could saturate the engagers and prevent their direct interactions with immune cells (Figures S4M and S4N). When incubated with 1 μg/ml recombinant SIRPα, the DKO$^{SIRP\alpha\text{-}E}$ cells were expeditiously killed by both NK cells and macrophages. This confirmed the necessity for direct cell-cell contact between engager cells and SIRPα on immune cells to inhibit their activation and thus their mechanism of action. When tested in C57BL/6 (B6) mouse DKO cells *in vitro*, the SIRPα engager reliably protected against NK cell and macrophage killing from both B6 mice and from humans (Figures S5A–S5C). We then injected WT, WT$^{SIRP\alpha\text{-}E}$, DKO, and DKO$^{SIRP\alpha\text{-}E}$ cells from B6 into fully allogeneic BALB/c recipients and performed ELISpot assays with splenocytes after 7 days (Figure S5D). As expected, there was a strong allogeneic immune response against B6 WT and WT$^{SIRP\alpha\text{-}E}$ cells (Figure S5E). The SIRPα engager, however, did not show any immunogenicity in DKO cells.

CellPress
OPEN ACCESS

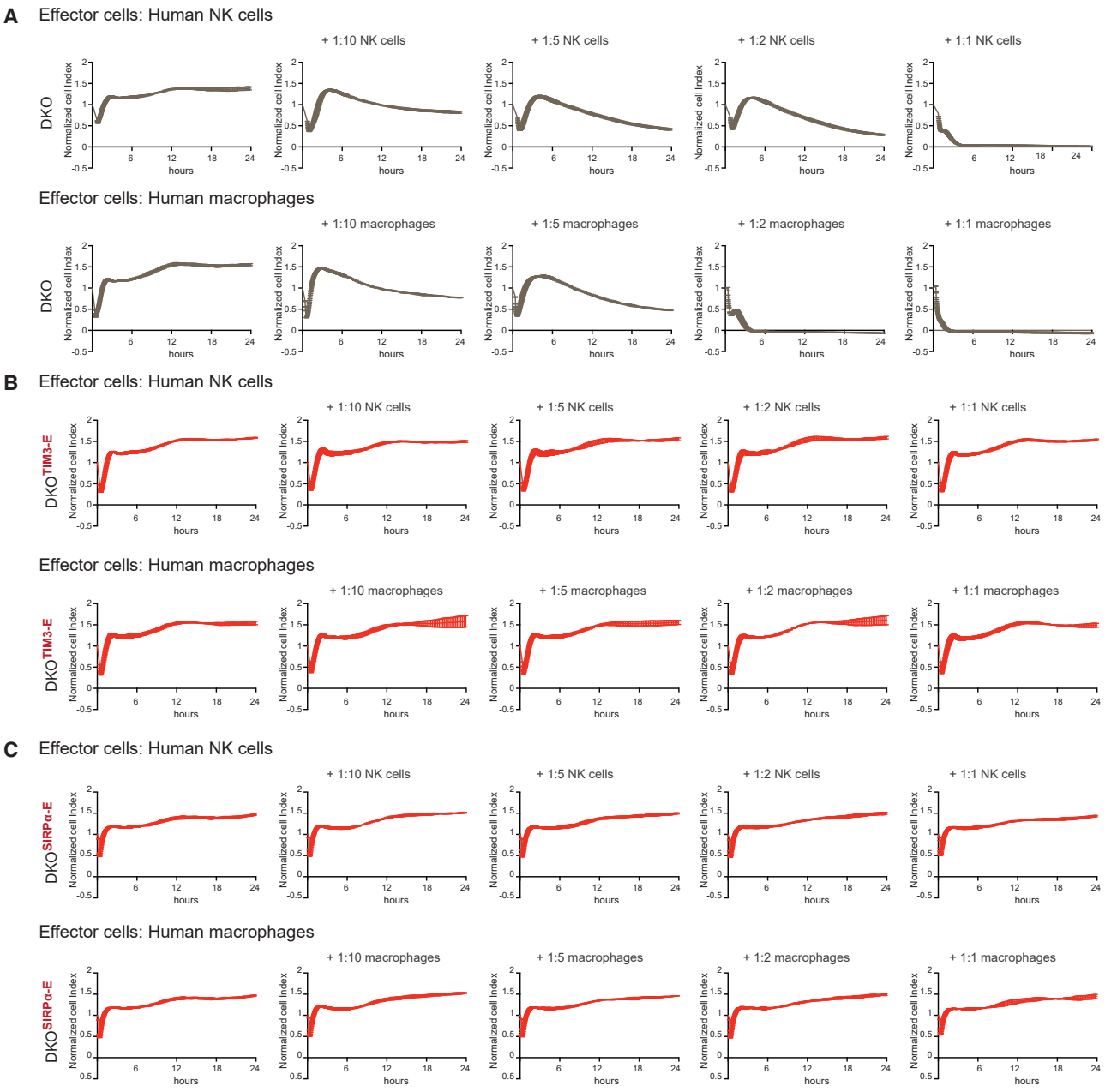

Figure 2. Engagers for TIM3 and SIRPα protect cells from NK cell and macrophage cytotoxicity

(A) DKO iECs were susceptible to NK cell and macrophage cytotoxicity and were killed increasingly quickly with increasing E:T ratios (mean ± SD per time point, n = 3).

(B and C) DKO iECs additionally expressing the synthetic engager for TIM3 (B) or SIRPα (C) were fully protected against both NK cell and macrophages killing (mean ± SD per time point, n = 3).

DKO$^{SIRP\alpha\text{-}E,CD64t}$ iECs are additionally protected from cytotoxic IgG

In solid organ transplantation, the relevance of antibody-mediated rejection became increasingly clear as cellular rejection could be managed more reliably with advanced immunosuppressive drug combinations. Allogeneic cell therapeutics are expected to face similar antibody problems when they are administered for long-term survival and in more immunocompetent patients. Expression of truncated CD64 (CD64t), a modified FcγRI receptor, was recently shown to capture cytotoxic IgG antibodies and protect the cells from both antibody-dependent cellular cytotoxicity (ADCC) as well as from complement-dependent cytotoxicity (CDC).[15] CD64t itself did not protect from NK cell killing (Figures 3A and 3B). We therefore aimed to combine antibody protection with the cellular immune evasion strategy by transducing the DKO$^{SIRP\alpha\text{-}E}$ iECs with lentiviral particles carrying the CD64t transgene. We first assessed whether the additional CD64t transgene would interfere with the SIRPα engager

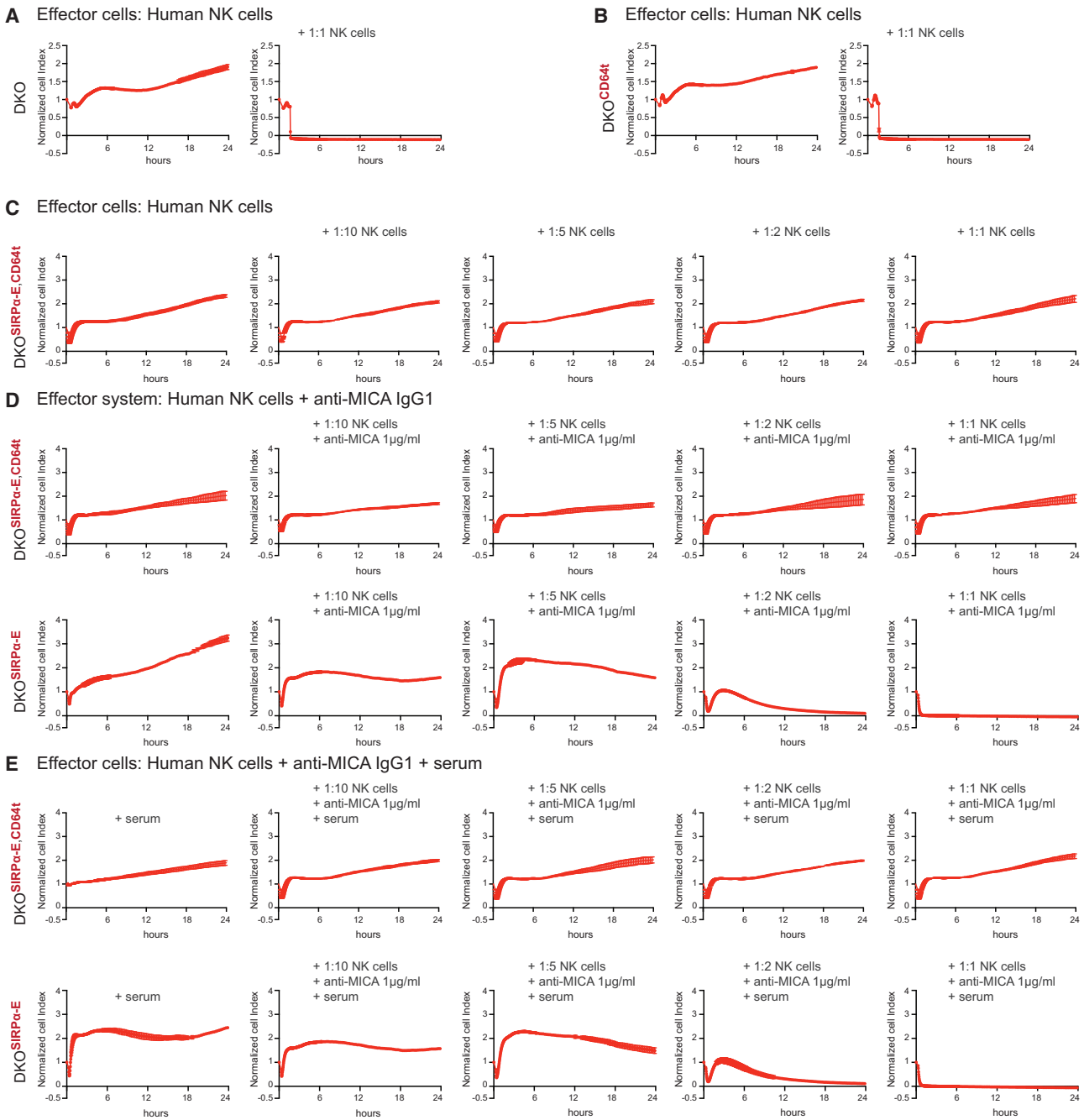

Figure 3. DKO iECs expressing the SIRPα engager and CD64t are fully protected from NK cells, ADCC, and CDC

(A and B) DKO iECs (A) and DKO^{CD64t} iECs (B) are both susceptible to NK cell killing (mean ± SD per time point, n = 3).

(C) DKO$^{SIRP\alpha\text{-}E,CD64t}$ iECs are protected from NK cell cytotoxicity, showing that the additional expression of CD64t does not mitigate the SIRPα immune checkpoint engager function (mean ± SD per time point, n = 3).

(D) A human IgG1 anti-MICA antibody was added to the assay to show that DKO$^{SIRP\alpha\text{-}E,CD64t}$ iECs are protected from NK cell cytotoxicity and NK cell ADCC. In contrast, DKO$^{SIRP\alpha\text{-}E}$ iECs lacking CD64t are susceptible to NK cell ADCC (mean ± SD per time point, n = 3).

(E) Human serum was added to the assay and DKO$^{SIRP\alpha\text{-}E,CD64t}$ iECs remained protected against NK cell cytotoxicity, NK cell ADCC, and also CDC. DKO$^{SIRP\alpha\text{-}E}$ iECs were killed (mean ± SD per time point, n = 3).

function to protect the cells from NK cell killing (Figure 3C). We found that DKO$^{SIRP\alpha\text{-}E,CD64t}$ iECs were still resistant to NK cell killing *in vitro*. We then added a human IgG1 antibody against the constitutively expressed major histocompatibility complex (MHC) class I-related sequence A (MICA) to induce ADCC. As expected, DKO$^{SIRP\alpha\text{-}E}$ iECs were killed increasingly quickly with increasing NK cell E:T ratios, but DKO$^{SIRP\alpha\text{-}E,CD64t}$ iECs were fully protected against antibody-mediated NK cell killing (Figure 3D). To additionally allow for CDC, we added serum to the assay (Figure 3E). DKO$^{SIRP\alpha\text{-}E,CD64t}$ iECs were still protected against both ADCC and CDC, whereas DKO$^{SIRP\alpha\text{-}E}$ iECs underwent killing. CD64t expression was therefore confirmed to protect engineered cells from cytotoxic IgG without interfering with the SIRPα engager function.

We next assessed the feasibility to engineer immune evasion using non-viral editing in a different iPSC line. Since iPSCs do not express HLA class II unless stimulated, we only targeted the B2M gene with Cas9 and guides and one HDR donor for both CD64t and the SIRPα engager (Figure S6A). The edited pool was then sorted for HLA I-depleted iPSCs with (B2M-KO$^{SIRP\alpha\text{-}E,CD64t}$) or without (B2M-KO) transgene expression (Figure S6B). The B2M-KO iPSCs were rapidly killed by both activated NK cells and macrophages, while the B2M-KO$^{SIRP\alpha\text{-}E,CD64t}$ iPSCs were protected (Figure S7A). In ADCC and CDC assays, unedited WT iPSCs were killed with different concentrations of a humanized anti-SSEA4 IgG1 antibody (Figures S7B and S7C). B2M-KO$^{SIRP\alpha\text{-}E,CD64t}$ iPSCs were protected from both types of antibody-mediated killing. These data show the simplicity to engineer iPSCs with effective immune evasion features.

DKO$^{SIRP\alpha\text{-}E,CD64t}$ iECs are protected against allogeneic cellular and antibody responses

The potential of DKO$^{SIRP\alpha\text{-}E,CD64t}$ iECs to survive the harshest allogeneic immune conditions was finally tested in maximally stringent immune environments. Engineered allogeneic cell therapeutics will eventually have to evade all of a patient's adaptive and innate immune attacks to allow for persistent efficiency. The FDA-approved anti-CD52 IgG1 antibody alemtuzumab (Campath) is well known for its high cytotoxicity and was chosen for *in vitro* testing because it was considered the highest bar to reach. To make our target cells susceptible to alemtuzumab, we used lentiviral particles to additionally express the alemtuzumab target CD52, which is not constitutively expressed on endothelial cells. The WT^{CD52} iECs were challenged with NK cells and macrophages and showed expedited killing whenever anti-CD52 IgG1 was added (Figure 4A). To allow for T cell allograft rejection, fresh peripheral blood mononuclear cells (PBMCs) from an HLA-A2-negative donor were primed *in vitro* with the HLA-A2$^+$ WT^{CD52} iECs for 14 days. Then, CD8$^+$ T cells were sorted and used for adaptive T cell cytotoxicity assays. We saw the typical *in vitro* T cell allo-rejection curve, which is slower than that for innate killing. When anti-CD52 IgG1 was added, T cell ADCC killed the WT^{CD52} targets more quickly. The WT^{CD52} iECs were additionally susceptible to CDC killing and were killed expeditiously when incubated in serum supplemented with anti-CD52 IgG1. In contrast, the DKO$^{SIRP\alpha\text{-}E,CD64t,CD52}$ iECs were protected from all allogeneic cellular immune responses as well as from ADCC and CDC (Figure 4B). We then tested the cells in a stringent allogeneic *in vivo* model. NSG-SGM3 mice were reconstituted with allogeneic CD34$^+$ hematopoietic stem cells and showed >40% of human CD45$^+$ cells among the overall CD45$^+$ population and >3% human CD3$^+$ cells among human CD45$^+$ cells when included in the study (Figure S5F). These humanized mice were additionally supplemented with one million human NK cells and three 1-mg doses of anti-CD52 IgG1 antibody (Figure 4C). The NK cells and the first dose of alemtuzumab were mixed and injected subcutaneously, together with 5×10^4 firefly luciferase$^+$ target cells, to maximize the cytotoxic potential of the antibody. All cell transplants were followed by BLI. The WT^{CD52} grafts vanished in just 1 day, most likely attributed to the highly cytotoxic nature of the anti-CD52 IgG1 and NK cells (Figure 4D). The DKO$^{SIRP\alpha\text{-}E,CD64t,CD52}$ grafts, however, showed unobstructed survival and thus confirmed their full protection from all allogeneic cellular and antibody responses (Figure 4E). Additionally, we tested immune evasiveness using a humanized IgG1 antibody against MICA. We injected 5×10^4 firefly luciferase$^+$ WT or DKO$^{SIRP\alpha\text{-}E,CD64t}$ iECs mixed with 1×10^6 human NK cells and 1 mg anti-MICA human IgG1 subcutaneously (Figure 4F). Another 1-mg dose of the anti-MICA human IgG1 was injected into the same site 2 days later. The WT grafts vanished over approximately 2 weeks, most likely due to the weaker cytotoxic potential of the anti-MICA antibody and the induction of the allogeneic adaptive rejection response (Figure 4G). The DKO$^{SIRP\alpha\text{-}E,CD64t}$ grafts were again protected from cellular alloimmunity as well as from antibody-mediated killing (Figure 4H).

DISCUSSION

The new area of engineered cells that will be used as living therapeutics is just beginning and expected to change the way we treat diseases. Immuno-oncology therapies have advanced the furthest and have shown encouraging early successes with autologous CAR-engineered primary T cells against hematologic cancers. Next-generation T cell products for solid tumors will require more extensive editing to increase their fitness and persistence and their homing capabilities and to improve their target specificity.[28] This will most likely require editing of iPSCs with subsequent differentiation of CD8$\alpha\beta$ CAR- or T cell receptor (TCR)-T cells, which has recently been achieved.[29] Since these induced pluripotent stem starter cells will be allogeneic, they will additionally require immune editing to make them fully immune evasive, which adds to the overall scope of gene engineering. We herein report an optimized and comprehensive immune evasion strategy that protects the engineered cells from all allogeneic adaptive and innate immune cells and antibody-mediated ADCC and CDC. Because of the full immune evasive nature of DKO$^{SIRP\alpha\text{-}E,CD64t}$ cells, cancer patients may not require lymphodepleting preconditioning at the currently used level or at all.

In autologous CAR T cell trials, cellular immune responses against the complementarity-determining and framework regions of the CAR variable domains[30] and retroviral vector epitopes have been observed and correlated with a lack of response.[31] The emergence of CAR-specific CD8$^+$ T cells[32] and of unique TCR Vβ gene clonotypes have been described.[33] Additionally, antibody responses against the CAR were detected in many patients in autologous CAR T cell trials against multiple

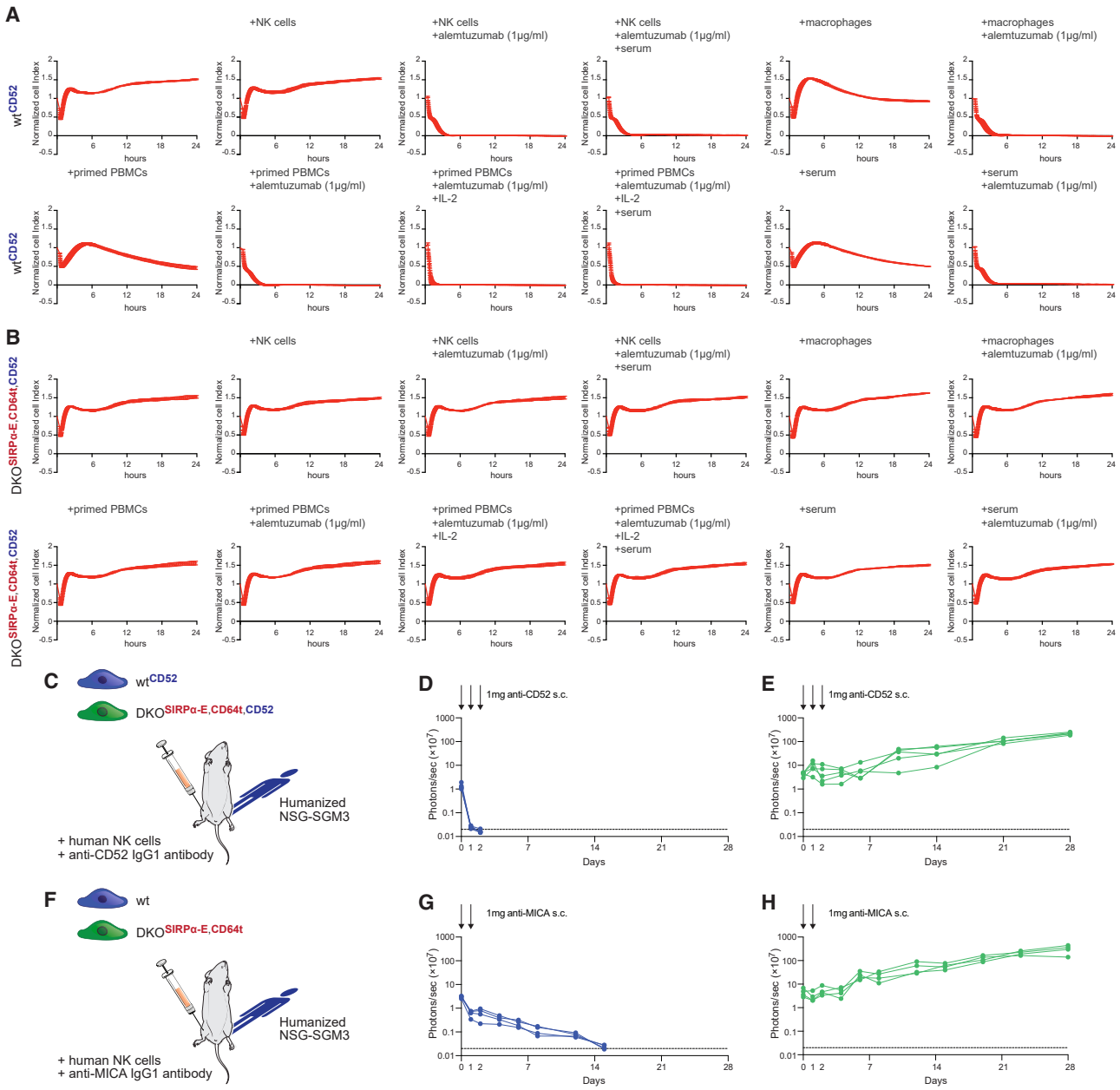

Figure 4. DKO iECs expressing the SIRPα engager and CD64t are fully protected against all allogeneic cellular and IgG responses

(A) WT^{CD52} iECs were challenged in increasingly hostile *in vitro* immune conditions. Effector immune cells were NK cells, macrophages, or allogeneic PBMCs that were primed against WT iECs. In some assays, serum was added to supply complement factors. In some assays, alemtuzumab was added to enable ADCC and CDC (mean ± SD per time point, n = 3). The WT^{CD52} iEC targets were rejected by the primed PBMCs and were killed in all assays including alemtuzumab (mean ± SD per time point, n = 3).

(B) $DKO^{SIRPα\text{-}E,CD64t,CD52}$ iECs were protected from all tested immune conditions and were thus protected from all allogeneic immune cells and cytotoxic IgG-mediated ADCC and CDC (mean ± SD per time point, n = 3).

(C) Luc^{+} WT^{CD52} iECs and $DKO^{SIRPα\text{-}E,CD64t,CD52}$ iECs were injected into allogeneic humanized mice supplemented with human NK cells and receiving 3 doses of the anti-CD52 IgG1 antibody alemtuzumab. All cells and antibody injections were administered into the subcutaneous tissue.

(D) The BLI signals for WT^{CD52} iECs vanished in just 1 day (all 5 mice are shown).

(E) The BLI signal for $DKO^{SIRPα\text{-}E,CD64t,CD52}$ iECs remained stable for the entire study (all 5 mice are shown).

(F) Luc^{+} WT iECs and $DKO^{SIRPα\text{-}E,CD64t}$ iECs were injected into allogeneic humanized mice supplemented with human NK cells and receiving 2 doses of a humanized anti-MICA IgG1 antibody. All cells and antibody injections were administered into the subcutaneous tissue.

(G) The BLI signals for WT iECs vanished over approximately 16 days (all four mice are shown).

(H) The BLI signal for $DKO^{SIRPα\text{-}E,CD64t}$ iECs remained stable for the entire study (all 4 mice are shown).

myeloma,[34] colorectal cancer,[35] and renal cell carcinoma.[31] The persistence of the CAR T cells in patients that developed antibodies against the CAR was low and patients relapsed. Repeat infusions of the same CAR T cell product increased the likelihood for antibody responses, and no patient with *de novo* antibodies against the CAR showed expansion of the CAR T cell product in the blood.[14] The first two trials using allogeneic anti-CD19 CAR T cells showed that more aggressive lymphodepletion was necessary to allow any proliferation of the CAR T cell product, but the persistence was still limited and efficacy inferior to comparable autologous products.[36] Extensive preconditioning increased the morbidity unacceptably and clearly shows that allogeneic immune-oncology products require immune evasion strategies to achieve efficacy and safety.

Regenerative medicine using allogeneic pluripotent stem cell-derived products is still mostly in preclinical phases but will face the same immune hurdle that solid organ transplants and CAR T cell products experience. Immune surveillance for allogeneic peptides is extremely thorough with rejection responses against cells with minor-[37], allo-[38], or neoantigens.[39] While a minor antigen mismatch was sufficient to reject homozygous MHC-matched iPSC-derived cardiomyocytes subcutaneously[40] and iPSC-derived neurons in the brain,[41] MHC-matched iPSC-derived retinal pigment epithelial cells transplanted into the subretinal space of the eye survived without any immune cell infiltrates.[42] Fully allogeneic iPSC-derived cardiomyocytes[43] or neurons[41] get vigorously rejected without heavy immunosuppression. Immune evasion edits could circumvent the allo-rejection problem for clinical translation. Diseases with an additional autoimmune component like Hashimoto's thyroiditis with pathognomonic autoantibody response require immune editing that includes protection from autoantibody IgG. Our concept presented herein comprehensively protects engineered cells from all immune cells and IgG.

Using synthetic immune cell checkpoint engagers with agonistic function, we were able to utilize inhibitory innate immune checkpoints not previously exploitable for the lack of specific natural ligands. Using a surface receptor molecular backbone with agonistic scFv, we could demonstrate binding capacity to their immune receptors and an inhibitory function in NK cells and macrophages that correlated with their receptor expression. The SIRPα engager effectively inhibited mouse and human NK cells and macrophages and is therefore not species restricted like SIRPα's natural ligand CD47.[17] Importantly, there was no measurable immune response against the SIRPα engager in DKO cells. In a previous study, our group similarly showed that no T cell responses can be induced when allogeneic proteins are expressed in MHC class I- and II-deficient cells.[39] Another recent study on hypoimmune human CAR T cells showed that administration of allogeneic HLA class I- and II-deficient CAR T cells does not prime T cells *in vivo*, and there is no cytotoxic response against CAR T populations with or without HLA.[7] The PD-1 engager was effective against T cells in this study and thus mitigated the adaptive immune response. The high fraction of PD-1 expressing cytotoxic T cells in our T cell experiments most likely contributed to the favorable results. The PD-1 engager was largely ineffective against innate immune cells, except for a sorted PD-1-expressing NK cell population. The LILRB1 engager in this study was similarly ineffective against NK cells as the natural ligand HLA-G in a recent publication.[2] Both LILRB family engagers successfully inhibited macrophage killing. The TIM3 engager is especially promising given its great efficacy *in vitro* and the high TIM3 expression levels on innate immune cells. This engager allows for the exploitation of an inhibitory immune checkpoint that is difficult to utilize via natural ligands. Mechanistically, our data show that direct engager-receptor interaction is necessary for the agonistic scFv to induce immune cell inhibition. Therefore, ectodomain shedding could mitigate immune checkpoint activation. There are reports of SIRPα shedding, but mainly from myotubes into motor axon synapses, where SIRPα acts as a presynaptic organizing molecule.[44] Shedding of the TIM-3 ectodomain has been described for human monocytes and T cells under certain inflammatory conditions.[45,46] Interestingly, TIM3 cannot be efficiently cleaved in the absence of an additional intracellular signaling event, and its overall biological significance is not fully understood. There have been no reports on LILRB1 or LILRB3 shedding.

At a time when iPSC-derived CD8αβ T cells,[47] pancreatic beta cells,[48] and retinal pigment epithelial cells[49] are ready for clinical translation, this immune evasion concept could contribute to their successful use in humans.

Limitations of the study

Although the SIRPα pathway in innate immune cells has been studied extensively and has repeatedly proven to be very effective for inhibiting cytotoxicity, the LILRB and TIM3 pathways are less well studied and understood. It remains unclear whether any of the theoretical mechanistic advantages of the SIRPα engager over CD47 are relevant in the context of immune evasion. Both have provided complete innate immune cell inhibition in this study and prior work. Also, different cell types have different levels of inherent immunogenicity, and implant locations come with their distinct local immune microenvironments for which certain engagers may be better suited than others or may require different expression levels. The fine-tuning of the immune evasion strategy needs to be performed on the specific cell products.

STAR★METHODS

Detailed methods are provided in the online version of this paper and include the following:

- KEY RESOURCES TABLE
- RESOURCE AVAILABILITY
  - Lead contact
  - Materials availability
  - Data and code availability
- EXPERIMENTAL MODEL AND STUDY PARTICIPANT DETAILS
  - Mice
- METHOD DETAILS
  - iPSC-derived ECs (iECs)
  - NK cell culture
  - Macrophage cell culture
  - iPSC cell culture
  - Transduction and sorting of iECs
  - Flow cytometry analysis

- Flow cytometry analysis for expression dynamics of the immune checkpoint engagers upon ligand binding
- Flow cytometry analysis of human immune cell reconstitution in humanized mice
- XCelligence killing assays
- Ex vivo T cell priming
- Survival analysis of human iECs using BLI
- ELISpot assays
- iPSC engineering

● QUANTIFICATION AND STATISTICAL ANALYSIS

SUPPLEMENTAL INFORMATION

Supplemental information can be found online at https://doi.org/10.1016/j.stem.2023.10.003.

ACKNOWLEDGMENTS

We thank V. Nguyen at the UCSF Parnassus Flow Cytometry Core for assistance with flow cytometry experiments.

AUTHOR CONTRIBUTIONS

A.G. and G.T. performed viral transductions and immune assays *in vitro* and *in vivo*. Y.Z., K.A.I., and L.G. performed CRISPR-Cas9 gene editing. S.M.P. and S.Z.R. performed flow cytometry. S.K. and M.O. supervised the iPSC experiments. All immune assays had been established by S.S. at UCSF. T.D. conceived and designed the study and wrote the manuscript. All the authors interpreted the data and read and provided feedback on the figures and manuscript.

DECLARATION OF INTERESTS

UCSF has filed patent applications that cover inventions of this study. Y.Z., K.A.I., S.M.P., S.Z.R., L.G., and M.O. are employees of Shinobi Therapeutics and own stock; S.K. and T.D. are founders of Shinobi Therapeutics and own stock. S.S. is currently an employee of Sana Biotechnology, Inc. and S.S. and T.D. own stock in Sana Biotechnology, Inc. No materials or funding was received from Sana Biotechnology, Inc. for use in this study

Received: December 19, 2022
Revised: August 23, 2023
Accepted: October 4, 2023
Published: November 2, 2023

REFERENCES

1. Helman, A., and Melton, D.A. (2021). A stem cell approach to cure type 1 diabetes. Cold Spring Harb. Perspect. Biol. *13*, a035741. https://doi.org/10.1101/cshperspect.a035741.
2. Hu, X., White, K., Olroyd, A.G., DeJesus, R., Dominguez, A.A., Dowdle, W.E., Friera, A.M., Young, C., Wells, F., Chu, E.Y., et al. (2023). Hypoimmune induced pluripotent stem cells survive long term in fully immunocompetent, allogeneic rhesus macaques. Nat. Biotechnol. https://doi.org/10.1038/s41587-023-01784-x.
3. Hu, X., Gattis, C., Olroyd, A.G., Friera, A.M., White, K., Young, C., Basco, R., Lamba, M., Wells, F., Ankala, R., et al. (2023). Human hypoimmune primary pancreatic islets avoid rejection and autoimmunity and alleviate diabetes in allogeneic humanized mice. Sci. Transl. Med. *15*, eadg5794. https://doi.org/10.1126/scitranslmed.adg5794.
4. DiNofia, A.M., and Grupp, S.A. (2021). Will allogeneic CAR T cells for CD19(+) malignancies take autologous CAR T cells 'off the shelf'? Nat. Rev. Clin. Oncol. *18*, 195–196. https://doi.org/10.1038/s41571-021-00485-1.
5. Depil, S., Duchateau, P., Grupp, S.A., Mufti, G., and Poirot, L. (2020). 'Off-the-shelf' allogeneic CAR T cells: development and challenges. Nat. Rev. Drug Discov. *19*, 185–199. https://doi.org/10.1038/s41573-019-0051-2.
6. Myers, J.A., and Miller, J.S. (2021). Exploring the NK cell platform for cancer immunotherapy. Nat. Rev. Clin. Oncol. *18*, 85–100. https://doi.org/10.1038/s41571-020-0426-7.
7. Hu, X., Manner, K., DeJesus, R., White, K., Gattis, C., Ngo, P., Bandoro, C., Tham, E., Chu, E.Y., Young, C., et al. (2023). Hypoimmune anti-CD19 chimeric antigen receptor T cells provide lasting tumor control in fully immunocompetent allogeneic humanized mice. Nat. Commun. *14*, 2020. https://doi.org/10.1038/s41467-023-37785-2.
8. Deuse, T., Hu, X., Gravina, A., Wang, D., Tediashvili, G., De, C., Thayer, W.O., Wahl, A., Garcia, J.V., Reichenspurner, H., et al. (2019). Hypoimmunogenic derivatives of induced pluripotent stem cells evade immune rejection in fully immunocompetent allogeneic recipients. Nat. Biotechnol. *37*, 252–258. https://doi.org/10.1038/s41587-019-0016-3.
9. Wang, B., Iriguchi, S., Waseda, M., Ueda, N., Ueda, T., Xu, H., Minagawa, A., Ishikawa, A., Yano, H., Ishi, T., et al. (2021). Generation of hypoimmunogenic T cells from genetically engineered allogeneic human induced pluripotent stem cells. Nat. Biomed. Eng. *5*, 429–440. https://doi.org/10.1038/s41551-021-00730-z.
10. Figueiredo, C., and Blasczyk, R. (2015). A future with less HLA: potential clinical applications of HLA-universal cells. Tissue Antigens *85*, 443–449. https://doi.org/10.1111/tan.12564.
11. Gornalusse, G.G., Hirata, R.K., Funk, S.E., Riolobos, L., Lopes, V.S., Manske, G., Prunkard, D., Colunga, A.G., Hanafi, L.A., Clegg, D.O., et al. (2017). HLA-E-expressing pluripotent stem cells escape allogeneic responses and lysis by NK cells. Nat. Biotechnol. *35*, 765–772. https://doi.org/10.1038/nbt.3860.
12. Zhao, L., Teklemariam, T., and Hantash, B.M. (2014). Heterelogous expression of mutated HLA-G decreases immunogenicity of human embryonic stem cells and their epidermal derivatives. Stem Cell Res. *13*, 342–354. https://doi.org/10.1016/j.scr.2014.08.004.
13. Xu, H., Wang, B., Ono, M., Kagita, A., Fujii, K., Sasakawa, N., Ueda, T., Gee, P., Nishikawa, M., Nomura, M., et al. (2019). Targeted disruption of HLA genes via CRISPR-Cas9 generates iPSCs with enhanced immune compatibility. Cell Stem Cell *24*, 566–578.e7. https://doi.org/10.1016/j.stem.2019.02.005.
14. Peraro, L., Bourne, C.M., Dacek, M.M., Akalin, E., Park, J.H., Smith, E.L., and Scheinberg, D.A. (2021). Incorporation of bacterial immunoevasins to protect cell therapies from host antibody-mediated immune rejection. Mol. Ther. *29*, 3398–3409. https://doi.org/10.1016/j.ymthe.2021.06.022.
15. Gravina, A., Tediashvili, G., Rajalingam, R., Quandt, Z., Deisenroth, C., Schrepfer, S., and Deuse, T. (2023). Protection of cell therapeutics from antibody-mediated killing by CD64 overexpression. Nat. Biotechnol. *41*, 717–727. https://doi.org/10.1038/s41587-022-01540-7.
16. Lanier, L.L. (2008). Up on the tightrope: natural killer cell activation and inhibition. Nat. Immunol. *9*, 495–502. https://doi.org/10.1038/ni1581.
17. Deuse, T., Hu, X., Agbor-Enoh, S., Jang, M.K., Alawi, M., Saygi, C., Gravina, A., Tediashvili, G., Nguyen, V.Q., Liu, Y., et al. (2021). The SIRPalpha-CD47 immune checkpoint in NK cells. J. Exp. Med. *218*, e20200839. https://doi.org/10.1084/jem.20200839.
18. Colonna, M., Navarro, F., Bellón, T., Llano, M., García, P., Samaridis, J., Angman, L., Cella, M., and López-Botet, M. (1997). A common inhibitory receptor for major histocompatibility complex class I molecules on human lymphoid and myelomonocytic cells. J. Exp. Med. *186*, 1809–1818. https://doi.org/10.1084/jem.186.11.1809.
19. Shiroishi, M., Kuroki, K., Ose, T., Rasubala, L., Shiratori, I., Arase, H., Tsumoto, K., Kumagai, I., Kohda, D., and Maenaka, K. (2006). Efficient leukocyte Ig-like receptor signaling and crystal structure of disulfide-linked HLA-G dimer. J. Biol. Chem. *281*, 10439–10447. https://doi.org/10.1074/jbc.M512305200.
20. Wu, G., Xu, Y., Schultz, R.D., Chen, H., Xie, J., Deng, M., Liu, X., Gui, X., John, S., Lu, Z., et al. (2021). LILRB3 supports acute myeloid leukemia

development and regulates T-cell antitumor immune responses through the TRAF2-cFLIP-NF-κB signaling axis. Nat. Cancer *2*, 1170–1184. https://doi.org/10.1038/s43018-021-00262-0.

21. Ndhlovu, L.C., Lopez-Vergès, S., Barbour, J.D., Jones, R.B., Jha, A.R., Long, B.R., Schoeffler, E.C., Fujita, T., Nixon, D.F., and Lanier, L.L. (2012). Tim-3 marks human natural killer cell maturation and suppresses cell-mediated cytotoxicity. Blood *119*, 3734–3743. https://doi.org/10.1182/blood-2011-11-392951.

22. Huang, Y.H., Zhu, C., Kondo, Y., Anderson, A.C., Gandhi, A., Russell, A., Dougan, S.K., Petersen, B.S., Melum, E., Pertel, T., et al. (2015). CEACAM1 regulates TIM-3-mediated tolerance and exhaustion. Nature *517*, 386–390. https://doi.org/10.1038/nature13848.

23. Das, M., Zhu, C., and Kuchroo, V.K. (2017). Tim-3 and its role in regulating anti-tumor immunity. Immunol. Rev. *276*, 97–111. https://doi.org/10.1111/imr.12520.

24. Yoshihara, E., O'Connor, C., Gasser, E., Wei, Z., Oh, T.G., Tseng, T.W., Wang, D., Cayabyab, F., Dai, Y., Yu, R.T., et al. (2020). Immune-evasive human islet-like organoids ameliorate diabetes. Nature *586*, 606–611. https://doi.org/10.1038/s41586-020-2631-z.

25. Benson, D.M., Jr., Bakan, C.E., Mishra, A., Hofmeister, C.C., Efebera, Y., Becknell, B., Baiocchi, R.A., Zhang, J., Yu, J., Smith, M.K., et al. (2010). The PD-1/PD-L1 axis modulates the natural killer cell versus multiple myeloma effect: a therapeutic target for CT-011, a novel monoclonal anti-PD-1 antibody. Blood *116*, 2286–2294. https://doi.org/10.1182/blood-2010-02-271874.

26. Soto-Pantoja, D.R., Terabe, M., Ghosh, A., Ridnour, L.A., DeGraff, W.G., Wink, D.A., Berzofsky, J.A., and Roberts, D.D. (2014). CD47 in the tumor microenvironment limits cooperation between antitumor T-cell immunity and radiotherapy. Cancer Res. *74*, 6771–6783. https://doi.org/10.1158/0008-5472.CAN-14-0037-T.

27. Oldenborg, P.A. (2013). CD47: a cell surface glycoprotein which regulates multiple functions of hematopoietic cells in health and disease. ISRN Hematol. *2013*, 614619. https://doi.org/10.1155/2013/614619.

28. Hou, A.J., Chen, L.C., and Chen, Y.Y. (2021). Navigating CAR-T cells through the solid-tumour microenvironment. Nat. Rev. Drug Discov. *20*, 531–550. https://doi.org/10.1038/s41573-021-00189-2.

29. Nishimura, T., Kaneko, S., Kawana-Tachikawa, A., Tajima, Y., Goto, H., Zhu, D., Nakayama-Hosoya, K., Iriguchi, S., Uemura, Y., Shimizu, T., et al. (2013). Generation of rejuvenated antigen-specific T cells by reprogramming to pluripotency and redifferentiation. Cell Stem Cell *12*, 114–126. https://doi.org/10.1016/j.stem.2012.11.002.

30. Lam, N., Trinklein, N.D., Buelow, B., Patterson, G.H., Ojha, N., and Kochenderfer, J.N. (2020). Anti-BCMA chimeric antigen receptors with fully human heavy-chain-only antigen recognition domains. Nat. Commun. *11*, 283. https://doi.org/10.1038/s41467-019-14119-9.

31. Lamers, C.H., Willemsen, R., van Elzakker, P., van Steenbergen-Langeveld, S., Broertjes, M., Oosterwijk-Wakka, J., Oosterwijk, E., Sleijfer, S., Debets, R., and Gratama, J.W. (2011). Immune responses to transgene and retroviral vector in patients treated with ex vivo-engineered T cells. Blood *117*, 72–82. https://doi.org/10.1182/blood-2010-07-294520.

32. Turtle, C.J., Hanafi, L.A., Berger, C., Gooley, T.A., Cherian, S., Hudecek, M., Sommermeyer, D., Melville, K., Pender, B., Budiarto, T.M., et al. (2016). CD19 CAR-T cells of defined CD4+:CD8+ composition in adult B cell ALL patients. J Clin Invest *126*, 2123–2138. https://doi.org/10.1172/JCI85309.

33. Jensen, M.C., Popplewell, L., Cooper, L.J., DiGiusto, D., Kalos, M., Ostberg, J.R., and Forman, S.J. (2010). Antitransgene rejection responses contribute to attenuated persistence of adoptively transferred CD20/CD19-specific chimeric antigen receptor redirected T cells in humans. Biol. Blood Marrow Transplant. *16*, 1245–1256. https://doi.org/10.1016/j.bbmt.2010.03.014.

34. Xu, J., Chen, L.J., Yang, S.S., Sun, Y., Wu, W., Liu, Y.F., Xu, J., Zhuang, Y., Zhang, W., Weng, X.Q., et al. (2019). Exploratory trial of a biepitopic CAR T-targeting B cell maturation antigen in relapsed/refractory multiple myeloma. Proc. Natl. Acad. Sci. USA *116*, 9543–9551. https://doi.org/10.1073/pnas.1819745116.

35. Hege, K.M., Bergsland, E.K., Fisher, G.A., Nemunaitis, J.J., Warren, R.S., McArthur, J.G., Lin, A.A., Schlom, J., June, C.H., and Sherwin, S.A. (2017). Safety, tumor trafficking and immunogenicity of chimeric antigen receptor (CAR)-T cells specific for TAG-72 in colorectal cancer. J. Immunother. Cancer *5*, 22. https://doi.org/10.1186/s40425-017-0222-9.

36. Benjamin, R., Graham, C., Yallop, D., Jozwik, A., Mirci-Danicar, O.C., Lucchini, G., Pinner, D., Jain, N., Kantarjian, H., Boissel, N., et al. (2020). Genome-edited, donor-derived allogeneic anti-CD19 chimeric antigen receptor T cells in paediatric and adult B-cell acute lymphoblastic leukaemia: results of two phase 1 studies. Lancet *396*, 1885–1894. https://doi.org/10.1016/S0140-6736(20)32334-5.

37. Hu, X., Kueppers, S.T., Kooreman, N.G., Gravina, A., Wang, D., Tediashvili, G., Schlickeiser, S., Frentsch, M., Nikolaou, C., Thiel, A., et al. (2020). The H-Y antigen in embryonic stem cells causes rejection in syngeneic female recipients. Stem Cells Dev. *29*, 1179–1189. https://doi.org/10.1089/scd.2019.0299.

38. Deuse, T., Wang, D., Stubbendorff, M., Itagaki, R., Grabosch, A., Greaves, L.C., Alawi, M., Grünewald, A., Hu, X., Hua, X., et al. (2015). SCNT-derived ESCs with mismatched mitochondria trigger an immune response in allogeneic hosts. Cell Stem Cell *16*, 33–38. https://doi.org/10.1016/j.stem.2014.11.003.

39. Deuse, T., Hu, X., Agbor-Enoh, S., Koch, M., Spitzer, M.H., Gravina, A., Alawi, M., Marishta, A., Peters, B., Kosaloglu-Yalcin, Z., et al. (2019). De novo mutations in mitochondrial DNA of iPSCs produce immunogenic neoepitopes in mice and humans. Nat. Biotechnol. *37*, 1137–1144. https://doi.org/10.1038/s41587-019-0227-7.

40. Kawamura, T., Miyagawa, S., Fukushima, S., Maeda, A., Kashiyama, N., Kawamura, A., Miki, K., Okita, K., Yoshida, Y., Shiina, T., et al. (2016). Cardiomyocytes derived from MHC-homozygous induced pluripotent stem cells exhibit reduced allogeneic immunogenicity in MHC-matched non-human primates. Stem Cell Rep. *6*, 312–320. https://doi.org/10.1016/j.stemcr.2016.01.012.

41. Morizane, A., Kikuchi, T., Hayashi, T., Mizuma, H., Takara, S., Doi, H., Mawatari, A., Glasser, M.F., Shiina, T., Ishigaki, H., et al. (2017). MHC matching improves engraftment of iPSC-derived neurons in non-human primates. Nat. Commun. *8*, 385. https://doi.org/10.1038/s41467-017-00926-5.

42. Sugita, S., Iwasaki, Y., Makabe, K., Kamao, H., Mandai, M., Shiina, T., Ogasawara, K., Hirami, Y., Kurimoto, Y., and Takahashi, M. (2016). Successful transplantation of retinal pigment epithelial cells from MHC homozygote iPSCs in MHC-matched models. Stem Cell Rep. *7*, 635–648. https://doi.org/10.1016/j.stemcr.2016.08.010.

43. Shiba, Y., Gomibuchi, T., Seto, T., Wada, Y., Ichimura, H., Tanaka, Y., Ogasawara, T., Okada, K., Shiba, N., Sakamoto, K., et al. (2016). Allogeneic transplantation of iPS cell-derived cardiomyocytes regenerates primate hearts. Nature *538*, 388–391. https://doi.org/10.1038/nature19815.

44. Umemori, H., and Sanes, J.R. (2008). Signal regulatory proteins (SIRPS) are secreted presynaptic organizing molecules. J. Biol. Chem. *283*, 34053–34061. https://doi.org/10.1074/jbc.M805729200.

45. Möller-Hackbarth, K., Dewitz, C., Schweigert, O., Trad, A., Garbers, C., Rose-John, S., and Scheller, J. (2013). A disintegrin and metalloprotease (ADAM) 10 and ADAM17 are major sheddases of T cell immunoglobulin and mucin domain 3 (Tim-3). J. Biol. Chem. *288*, 34529–34544. https://doi.org/10.1074/jbc.M113.488478.

46. Hansen, J.A., Hanash, S.M., Tabellini, L., Baik, C., Lawler, R.L., Grogan, B.M., Storer, B., Chin, A., Johnson, M., Wong, C.H., et al. (2013). A novel soluble form of Tim-3 associated with severe graft-versus-host disease. Biol. Blood Marrow Transplant. *19*, 1323–1330. https://doi.org/10.1016/j.bbmt.2013.06.011.

47. Iriguchi, S., Yasui, Y., Kawai, Y., Arima, S., Kunitomo, M., Sato, T., Ueda, T., Minagawa, A., Mishima, Y., Yanagawa, N., et al. (2021). A clinically applicable and scalable method to regenerate T-cells from iPSCs for off-the-shelf T-cell immunotherapy. Nat. Commun. *12*, 430. https://doi.org/10.1038/s41467-020-20658-3.

48. Hogrebe, N.J., Maxwell, K.G., Augsornworawat, P., and Millman, J.R. (2021). Generation of insulin-producing pancreatic beta cells from multiple human stem cell lines. Nat. Protoc. *16*, 4109–4143. https://doi.org/10.1038/s41596-021-00560-y.

49. Sharma, R., Khristov, V., Rising, A., Jha, B.S., Dejene, R., Hotaling, N., Li, Y., Stoddard, J., Stankewicz, C., Wan, Q., et al. (2019). Clinical-grade stem cell-derived retinal pigment epithelium patch rescues retinal degeneration in rodents and pigs. Sci. Transl. Med. *11*, eaat5580. https://doi.org/10.1126/scitranslmed.aat5580.

STAR★METHODS

KEY RESOURCES TABLE

REAGENT or RESOURCE	SOURCE	IDENTIFIER
Antibodies		
humanized anti-CD52 IgG1	ichorbio	Cat# ICH4002
humanized anti-MICA IgG1	Creative Biolabs	Cat# TAB-0799CL
APC mouse anti-human CD3 antibody	BD Biosciences	clone SP34-2, Cat# 557597; RRID:AB_398626
isotype-matched control APC mouse IgG1κ antibody	BD Biosciences	clone MOPC-21, Cat# 550854; RRID:AB_398467
BV421 mouse anti-human CD8 antibody	Biolegend	clone SK1, Cat# 344748; RRID:AB_2629583
isotype-matched control BV421 mouse IgG1κ antibody	Biolegend	clone MOPC-21, Cat# 400157; RRID:AB_10897939
Bacterial and virus strains		
Lentiviruses for the engagers	GenTarget	Custom orders
Lentivirus for firefly luciferase	GenTarget	Cat# LVP325
Chemicals, peptides, and recombinant proteins		
Human VEGF	PeproTech	Cat# 100-20
Human FGFb	PeproTech	Cat# 100-18B
Y-27632	Sigma-Aldrich	Cat# Y0503, CAS 129830-38-2
SB 431542	Sigma-Aldrich	Cat# S4317, CAS 301836-41-9
Human IL-2	PeproTech	Cat# 200-02
Human M-CSF	PeproTech	Cat# 300-25
biotinylated human SIRPα protein	AcroBiosystems	Cat# SIA-H82A3
biotinylated human LILRB1 protein	AcroBiosystems	Cat# CDJ-H82F7
biotinylated human TIM3 protein	AcroBiosystems	Cat# TM3-H82E7
APC Streptavidin	Biolegend	Cat# 405207
Experimental models: Cell lines		
Human Episomal Cas9 iPSC Cell Line	Gibco	Cat# A33124
Experimental models: Organisms/strains		
NOD.Cg-*Prkdc*^{scid} *Il2rg*^{tm1Wjl} Tg(CMV-IL3,CSF2,KITLG)1Eav/MloySzJ	Jackson Laboratories	Strain 013062
Ff-I01s04 QHJI iPSC	Kyoto University	N/A
Recombinant DNA		
HDR donor template	Genscript	N/A
Software and algorithms		
RTCA software	ACEA	N/A
Prism	GraphPad	v9.5.1
Aura Image software	Spectral Instruments	N/A

RESOURCE AVAILABILITY

Lead contact

Further information and requests for resources and reagents should be directed to and will be fulfilled by the lead contact, Tobias Deuse (Tobias.Deuse@ucsf.edu).

Materials availability

All the materials will be available upon request from the lead contact under material transfer agreement with UCSF and Kyoto University.

Data and code availability

This manuscript did not generate any new code. All data reported in this paper will be shared by the lead contact upon request. Any additional information required to reanalyze the data reported in this paper is available from the lead contact upon request.

EXPERIMENTAL MODEL AND STUDY PARTICIPANT DETAILS

Mice

Female humanized NSG-SGM3 (NOD.Cg-*Prkdc*^{scid} *Il2rg*^{tm1Wjl} Tg(CMV-IL3,CSF2,KITLG)1Eav/MloySzJ, 013062) reconstituted with human CD34$^+$ hematopoietic stem cell were purchased from the Jackson Laboratories (Sacramento, CA). Humanized mice were not thymectomized, received human CD34$^+$ cells at 12 weeks of age, and were included into study groups 6 – 8 weeks after humanization. The number of animals used in the experiments is presented in each figure. Mice received humane care in compliance with the Guide for the Principles of Laboratory Animals. Mice were housed in 12-hour light-dark cycles with humidity between 30-70% at ambient temperature of 20-26 degrees Celsius. The study and control animals were housed in the same room. The animal facility is a specific pathogen-free facility. Animal experiments were approved by the University of California, San Francisco (UCSF) Institutional Animal Care and Use Committee and performed according to local guidelines.

METHOD DETAILS

iPSC-derived ECs (iECs)

DKO endothelial cells were differentiated from *B2M*$^{-/-}$ *CIITA*$^{-/-}$ iPSCs as described previously.[8] Then, iECs were maintained in Endothelial Cell Basal Medium 2 (PromoCell, Heidelberg, Germany) plus supplements, 10% FCS hi (Gibco), 1% pen/strep, 25 ng/ml VEGF (PeproTech), 2 ng/ml FGFb (PeproTech), 10 μM Y-27632 (Sigma-Aldrich), and 1 μM SB 431542 (Sigma-Aldrich). TrypLE (Gibco) was used for passaging the cells 1:3 every 3 to 4 days. For luciferase transduction, 1 x 10^5 iECs were plated in a 6-well and grown overnight at 37° C with 5% CO_2. Medium was changed the next day and 200 μl of Fluc lentiviral particles expressing luciferase II gene under re-engineered EF1a promotor (Gentarget) was added. After 36 h, 1 ml of cell medium was added. After another 24 h, complete medium change was performed. Two days later, luciferase expression was confirmed by adding D-luciferin (Promega, Madison, WI). Signals were quantified in p/s/cm^2/sr.

NK cell culture

Human primary NK cells were purchased from Stemcell Technologies (70036, Vancouver, Canada) and were cultured in RPMI-1640-GlutaMax (Gibco) plus 10% FCS hi, 1x non-essential amino acids (HyClone), and 1% pen/strep before performing the assays. NK cells were stimulated with IL-2 (Peprotech) 1μg/mL overnight before and during assays.

Macrophage cell culture

Human primary macrophages were purchased from Stemcell Technologies (70042, Vancouver, Canada) and were cultured in RPMI-1640-GlutaMax (Gibco) plus 10% FCS hi and 1% pen/strep before performing the assays.

iPSC cell culture

The Ff-I01s04 iPSCs were provided by Kyoto University. iPSCs were cultured in StemFit Basic04 complete (amsbio) on cellware coated with iMatrix-511 silk (Iwai North America). Cells were lifted with 0.5x TrypLE Select (Gibco) or Accutase (Innovative Cell Technologies) and 10μM Y-27632 (FujiFilm WAKO) was included for 24h post-subculture.

Transduction and sorting of iECs

In a pre-coated 12-well plate, human DKO iECs were plated at a density of 5 x 10^4 in cell-specific media and then incubated overnight at 37°C at 5% CO_2. The next day, cells were incubated overnight at 37°C, 5% CO_2 with lentiviral particles carrying a transgene for one of the 5 engager molecules (Gentarget, custom products) at a multiplicity of infection of 10 (Table S1). Protamine sulfate (1μg/ml) was added to the media and the plate was centrifuged at 200 g for 30 min prior to the overnight incubation. Cell populations were sorted on FACSAria (BD Biosciences) using RFP fluorescence.

Flow cytometry analysis

To assess binding capacity of DKO-Engager cells with their respective immune checkpoint receptors, biotinylated human SIRPα protein with mouse IgG2a Fc and Avitag (Cat.no. SIA-H82A3, AcroBiosystems), biotinylated human LILRB1 protein with Fc and Avitag (Cat.no. CDJ-H82F7, AcroBiosystems), biotinylated human TIM3 protein with Avitag (Cat.no. TM3-H82E7, AcroBiosystems) were used with APC Streptavidin (Cat.no. 405207, Biolegend). DKO iECs served as controls. Cells were analyzed on the LSR Fortessa (BD Bioscience) and results were expressed as fold-change to APC Streptavidin.

Flow cytometry analysis for expression dynamics of the immune checkpoint engagers upon ligand binding

To assess the expression upon ligand binding of SIRPα engager on iEC DKO$^{SIRPa\text{-}E}$ cells, iEC DKO$^{SIRPa\text{-}E}$ cells were incubated 3h with biotinylated human SIRPα protein with mouse IgG2a Fc and Avitag (Cat.no. SIA-H82A3, AcroBiosystems), or human macrophages

and the expression of the SIRPα engager was determined before and after ligand binding. To assess the expression upon ligand binding of LILRB1 engager on iEC DKO$^{LILRB1\text{-}E}$ cells, DKO$^{LILRB1\text{-}E}$ cells were incubated 3h with human macrophages and the expression of the LILRB1 engager was determined before and after ligand binding. Similarly, DKO$^{TIM3\text{-}E}$ cells were incubated 3h with human NK cells and the expression of the TIM3 engager was determined before and after ligand binding. Engager surface expression was quantified using AF-647 anti-rabbit G4S linker antibody (Cat.no.69782, Clone E7O2V, Cell Signaling) and matching AF-647 isotype control rabbit IgG (Cat.no.02-6102, Thermo Fisher). Cells were analyzed on the LSR Fortessa (BD Bioscience).

Flow cytometry analysis of human immune cell reconstitution in humanized mice

Splenocytes from female humanized NSG-SGM3 mice were stained for human CD45 with PE anti-human CD45 antibody (cat.no. 304039, Clone HI30, Biolegend) and matching isotype control PE Mouse IgG1, κ (cat.no. 981804, clone MOPC-21, Biolegend); PerCP conjugated anti-human CD19 (cat.no. 302228, clone HIB19, Biolegend) and matching isotype control PerCP Mouse IgG1, κ (cat.no. 400148, clone MOPC-21, Biolegend); AF488 anti-human CD3 (cat.no. 300415, clone UCHT-1, Biolegend) and isotype control AF488 Mouse IgG1, κ (cat.no. 400129, clone MOPC-21, Biolegend); BV605 anti-human CD33 (cat.no. 366612, clone P67.6, Biolegend) and isotype control BV605 Mouse IgG1, κ (cat.no. 400162, clone MOPC-21, Biolegend); PerCP/Cy5.5 anti -human CD56 (cat.no. 304626, clone MEM-188, Biolegend) and matching isotype control PerCP/Cy5.5 Mouse IgG2a, κ (cat.no. 400251, clone MPOC-173, Biolegend). Cells were analyzed on the LSR Fortessa (BD Bioscience) and results were expressed as fold-change to isotype controls.

XCelligence killing assays

Real-time killing assays were performed on the XCelligence SP platform and MP platform (ACEA Biosciences, San Diego, CA.). Special 96-well E-plates (ACEA Biosciences) coated with 0.1% gelatin (Sigma-Aldrich) were used for iECs, and Easy iMatrix-511 Silk (Iwait North America) for iPSCs. A total of 4 × 10^4 human iECs or 2 × 10^4 human iPSCs were plated in 100 μl medium. After the cell index reached stable levels >0.7, human NK cells, macrophages, or PBMCs were added at different E:T ratios. Alternatively, 50 μl blood-type compatible human serum was added. For ADCC or CDC assays, the following antibodies were used and added after mixing with the NK cells in 50 μl medium or in the serum as indicated: humanized anti-CD52 IgG1 (alemtuzumab, ichorbio, cat.no. ICH4002), humanized anti-MICA IgG1 (Creative Biolabs, cat.no. TAB-0799CL) or humanized anti-SSEA-4 IgG1 (Creative Biolabs, cat.no. HPAB-N0258-YC). As a negative control, cells were treated with 2% Triton X-100 in medium. Data were standardized and analyzed with the RTCA software (ACEA).

Ex vivo T cell priming

Blood from an HLA-A2-negative donor was collected and PBMCs were obtained after Ficoll separation. The PBMCs were primed by co-culturing 5 × 10^5 HLA-A2-positive wt iEC cells and 1 × 10^6 PBMC in a gelatin-coated flasks. The media, which consisted of a 1:1 mixture of endothelial cell medium and PBMC medium, was changed every 3 days. After 14 days, the cells in suspension were harvested and sorted using an APC mouse anti-human CD3 antibody (clone SP34-2, catalog no. 557597, BD Biosciences, conc. 0.01 mg/ml) together with the isotype-matched control APC mouse IgG1κ antibody (clone MOPC-21, catalog no. 550854, BD Biosciences, conc. 0.01 mg/ml), and a BV421 mouse anti-human CD8 antibody (clone SK1, catalog no. 344748, Biolegend, conc. 0.005 mg/ml) together with the isotype-matched control BV421 mouse IgG1κ antibody (clone MOPC-21, catalog no. 400157, Biolegend, conc. 0.005 mg/ml). The $CD3^+CD8^+$ cells were sorted using a FACS Aria flow cytometer (BD Biosciences) and used for real-time XCelligence killing assays.

Survival analysis of human iECs using BLI

A total of 5 × 10^4 wt or engineered iECs were injected subcutaneously into humanized NSG-SGM3 mice mixed together with one million human NK cells that were stimulated with IL-2 1μg/ml for 24 h before being injected into the animals and 1 mg of alemtuzumab or anti-MICA IgG1. On the one (anti-MICA) or two (alemtuzumab) subsequent days, 1 mg doses were injected subcutaneously into the vicinity of the cell transplants. All injected cells were Luc^+. For imaging, D-luciferin firefly potassium salt (375 mg/kg; Biosynth AG, Staad, Switzerland) was dissolved in PBS (pH 7.4, Gibco) and 250 μl was injected intraperitoneally in anesthetized mice. Animals were imaged in the AMI HT (Spectral Instruments Imaging). Region of interest (ROI) bioluminescence was quantified in units of maximum photons per second per centimeter square per steradian (p/s/cm^2/sr). The maximum signal from an ROI was measured using Aura Image software (Spectral Instruments).

ELISpot assays

For uni-directional ELISpot assays, splenocytes of BALB/c recipient were isolated 7 days after cell injections, and splenocytes were plated on ELISpot plates as recipient cells. Donor cells were treated with mitomycin (50 μg/ ml for 30 min, Sigma-Aldrich) and used as stimulator cells. A total of 1 × 10^5 stimulator cells were incubated with 1 × 10^6 recipient responder PBMCs for 24 h, and IFN-γ spot frequencies (BD Biosciences) were enumerated using an ELISpot plate reader.

iPSC engineering

Guide RNA targeting the B2M locus was purchased from Synthego (Redwood City, CA), and resuspended in TE at a concentration of 100 μM, aliquoted and stored at -80 °C. Knock-in donor template plasmid was synthesized by Genscript (Piscataway, NJ), and

resuspend in TE at a final concentration of 1 μg/μl. To make RNP, 20 pmol Cas9 from Aldeveron (Fargo, ND) and 100 pmol gRNA was mixed in complete nucleofection buffer P3 (Lonza, Basel, Switzerland), and incubated at room temperature for 10 min prior to adding 0.5-1 μg of donor template. Immediately prior to electroporation, Ff-I01s04 iPSCs were dissociated into single cell suspension and resuspended in complete nucleofection buffer P3 (Lonza) using 10 μl buffer per 0.5-1×10^6 viable cells. Cells were mixed with RNP and electroporated in a Lonza 4D-Nucleofector with program CA-137. Immediately after electroporation, 80 μl of cell culture medium was added to the well, and cells were recovered at 37 °C for 5 min. Edited iPSC cells were replated in culture medium with 10 μM Y-27632 (FujiFilm, Minato City, Japan) and 0.25 μg/cm^2 iMatrix-511 SILK (Amsbio, Cambridge, MA). B2M-KO iPSCs were selected by depleting B2M positive cells from edited iPSC using an anti-B2M antibody (cat.no. 316306, Biolegend, PE conjugated) and anti-PE microbeads (cat.no. 130-048-801, Miltenyi) per manufacturer protocol. B2M-KO$^{SIRP\alpha\text{-}E,CD64t}$ iPSCs were sorted on FACSAria (BD Biosciences) using the following antibodies under manufacturer instructions: anti-human B2M-PE-Cy7 (cat.no. 400126, Biolegend), anti-human CD64-PE (cat.no. 305008, Biolegend), anti-myc tag-Alexa Fluro 647 (cat.no. ab223895, Abcam). The edited iPSCs were further phenotyped using flow cytometry with the above antibodies, and also a custom biotinylated anti-G4S-linker F(ab')2 antibody (Cell Signaling Technologies, custom order) with Streptavidin-Brilliant Violet 711 (cat.no. 405241, Biolegend). B2M-KO without transgene expression and B2M-KO$^{SIRP\alpha\text{-}E,CD64t}$ with transgene expression were used in assays.

QUANTIFICATION AND STATISTICAL ANALYSIS

All data are expressed as mean ± SD. The two-tailed Student's *t* test was used to compare two groups and statistical analyses of three or more groups were performed using a one-way ANOVA followed by the Bonferroni post hoc test. GraphPad Prism 9 was used for all analyses. Animals were randomly assigned to experimental groups. The number of animals per experimental group is presented in each figure.

Cell Stem Cell, Volume *30*

Supplemental Information

Synthetic immune checkpoint engagers protect HLA-deficient iPSCs and derivatives from innate immune cell cytotoxicity

Alessia Gravina, Grigol Tediashvili, Yueting Zheng, Kumiko A. Iwabuchi, Sara M. Peyrot, Susan Z. Roodsari, Lauren Gargiulo, Shin Kaneko, Mitsujiro Osawa, Sonja Schrepfer, and Tobias Deuse

PD-1 engager	MALPVTALLLPLALLLHAARPEQKLISEEDLDIQMTQSPSSLSASVGDRVTITCQA SQSPNNLLAWYQQKPGKAPKLLIYGASDLPSGVPSRFSGSGSGTDFTLTISSLQ PEDFATYYCONNYYVGPVSYAFGGGTKVEIKGGGGSGGGGSGGGGSQVQLV QSGAEVKKPGASVKVSCKVSGYSLSKYDMSWVRQAPGKGLEWMGIIYTSGYT DYAQKFQGRVTMTEDTSTDTAYMELSSLRSEDTAVYYCATGNPYYTNGFNSW GQGTLVTVSSTTTPAPRPPTPAPTIASQPLSLRPEACRPAAAVHTRGLDFACDA AVLVLLVIVIISLIVLVVIW
LILRB1 engager	MALPVTALLLPLALLLHAARPEQKLISEEDLEQSLEESGGGLVKPGASLTVTCAV SGFSLNSYAITWVRQAPGKGLEYIGYIDTGASITDYASWAKGRFTISKTSSTTVTL EMTSLTDADTATYFCARGFSMFKLWGPGTLVTISSGGGGSGGGGSGGGGSEL DLTQTPSSVSAAVGGTVTISCQASQSVYGNNRLAWYHQKPGQPPKRLIYLASTL DSGVPSRFKGAGSGTQFTLTISDLECDDAATYYCAGGYAGNFNAFGGGTEVEI KTTTPAPRPPTPAPTIASQPLSLRPEACRPAAAVHTRGLDFACDAAVLVLLVIVIIS LIVLVVIW
TIM3 engager	MALPVTALLLPLALLLHAARPEQKLISEEDLQMQLVQSGGEVKKPGASVKVSCK TSGYRFTSYGISWVRQAPGQGLEWMGWISGYNGETNYAETLQGRLTLTTDTST STAYMELGSLRPDDTAVYYCTRDGHSPYFDYWGQGTLVTVSSGGGGSGGGG SGGGGSQAVLTQPASVSGSPGQSVTISCTGTSSDVGGYNYVSWYQQHPGKAP KLMIYEVSKRPSGIPERFSGSNSGNTATLTISRVEAGDEADYYCQVWDSSSDH WVFGRGTKLTVLTTTPAPRPPTPAPTIASQPLSLRPEACRPAAAVHTRGLDFAC DAAVLVLLVIVIISLIVLVVIW
SIRPα engager	MALPVTALLLPLALLLHAARPEQKLISEEDLQVQLVESEGGLVQPGGSLRLSCAA SGFTFSSYEMNWVRQAPGKGLEWVSYISSSGSTIYYADSVKGRFTISRDNAKN SLYLQMNSLRAEDTAVYYCAREAKGYYYGMDVWGQGTTVTVSSGGGGSGGG GSGGGGSQPVLTQSPSVSVSPGQTASITCSGDKLGDTYACWYQQKPGQSPVL VIYQDTKRPSGIPERFSGSNSGNTATLTISGTQAMDEADYYCQAWDSSTVVFG GGTKLTVLTTTPAPRPPTPAPTIASQPLSLRPEACRPAAAVHTRGLDFACDAAVL VLLVIVIISLIVLVVIW
LILRB3 engager	MALPVTALLLPLALLLHAARPEQKLISEEDLEVQLLESGGGLVQPGGSLRLSCAA SGFTFSSYAMSWVRQAPGKGLEWVSAISGSGGSTYYADSVKGRFTISRDNSKN TLYLQMNSLRAEDTAVYYCARRKKRERGFSGNDPVGAIDVWGQGTLVTVSSG GGGSGGGGSGGGGSQSVLTQPPSASGTPGQRVTISCTGSSSNIGAGYDVHW YQQLPGTAPKLLIYGNTNRPSGVPDRFSGSKSGTSASLAISGLRSEDEADYYCS AWDDSLSGVVFGGGTKLTVLGTTTPAPRPPTPAPTIASQPLSLRPEACRPAAAV HTRGLDFACDAAVLVLLVIVIISLIVLVVIW

Table S1: *Sequences of immune checkpoint engagers*, related to STAR Methods**.**

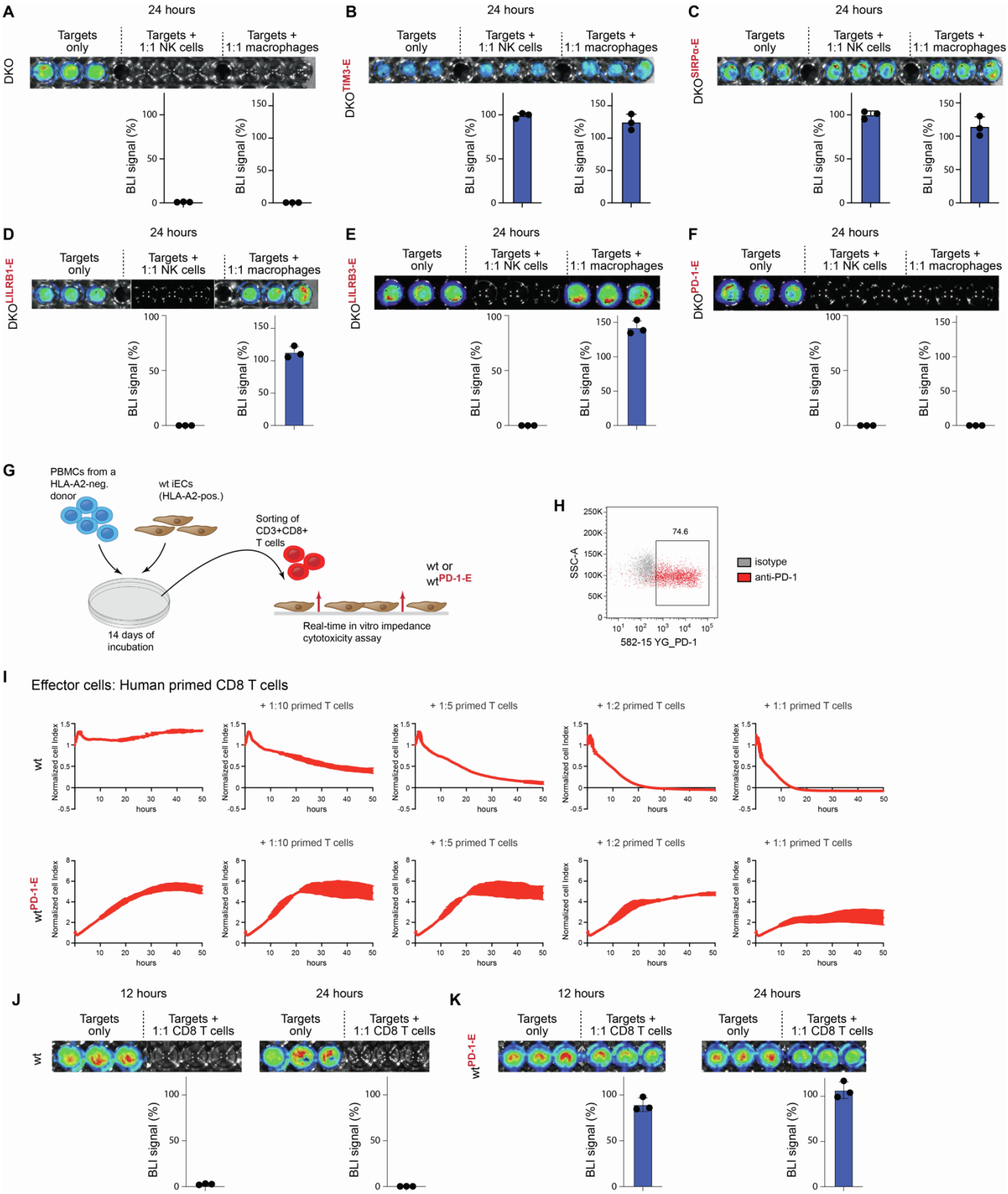

Figure S1: *Different engagers affect different effector cell populations.* Related to Figure 2.
(A) Luc^{+} DKO iECs were susceptible to NK cell and macrophage cytotoxicity and were killed within 24 hours (mean ± SD, n=3).

(B-C) Luc^+ DKO iECs additionally expressing the synthetic engager for TIM3 (B), or SIRPα (C) were fully protected from NK cell and macrophages killing (mean ± SD, n=3).
(D-E) Luc^+ $DKO^{LILRB1\text{-}E}$ iECs (D) and $DKO^{LILRB3\text{-}E}$ iECs (E) were killed by NK cells within 24 hours but were protected from macrophage killing (mean ± SD, n=3).
(F) Luc^+ $DKO^{PD\text{-}1\text{-}E}$ iECs were susceptible to both NK cell and macrophage cytotoxicity (mean ± SD, n=3).
(G) Fresh PBMCs from an HLA-A2-negative donor were incubated with HLA-A2-positive wt iECs for 14 days. Then, cells were recovered and sorted for $CD3^+CD8^+$ cells and used as effector cells in cytotoxicity assays with HLA-A2-positive wt or $wt^{PD\text{-}1\text{-}E}$ iECs.
(H) The expression of PD-1 on $CD3^+CD8^+$ cells is shown by flow cytometry (representative picture).
(I-K) While Luc+ wt iECs underwent T cell killing in an E:T ratio-dependent kinetics, $wt^{PD\text{-}1\text{-}E}$ iECs were protected in impedance (I) and BLI (J and K) assays (mean ± SD per time point, n=3).

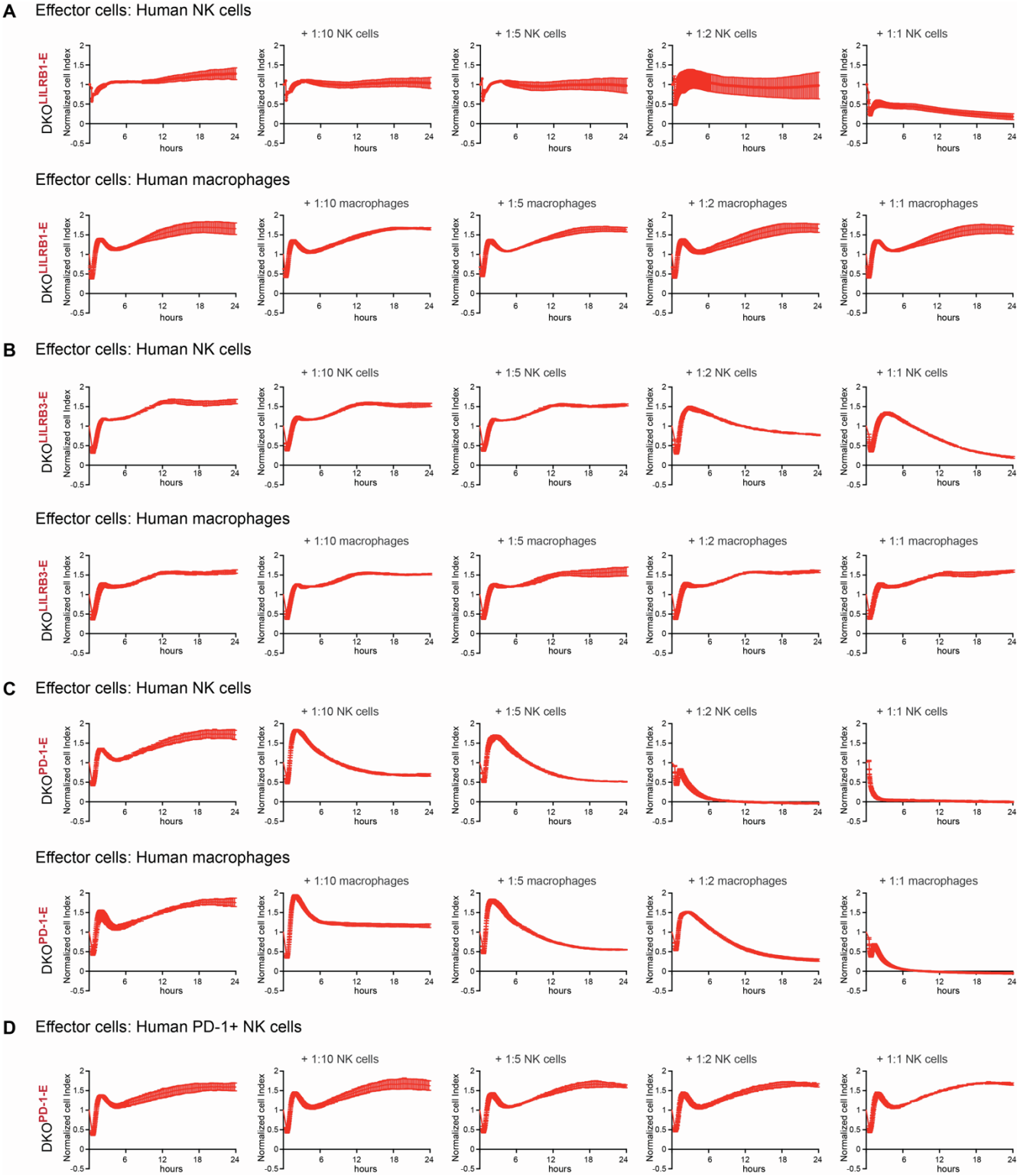

Figure S2: *Engagers for LILRB1, LILRB3, and PD-1 are insufficient to protect DKO cells from both NK cells and macrophages.* Related to Figure 2.

(A-B) DKO$^{LILRB1\text{-}E}$ iECs (A) and DKO$^{LILRB3\text{-}E}$ iECs (B) remained susceptible to NK cell cytotoxicity, although they showed protection from macrophage killing (mean ± SD per time point, n=3).

(C) DKO$^{PD\text{-}1\text{-}E}$ iECs were susceptible to both NK cell and macrophage cytotoxicity (mean ± SD per time point, n=3).
(D) When using PD-1^{+} NK cells as effector cells, then DKO$^{PD\text{-}1\text{-}E}$ iECs were protected from cytotoxicity (mean ± SD per time point, n=3).

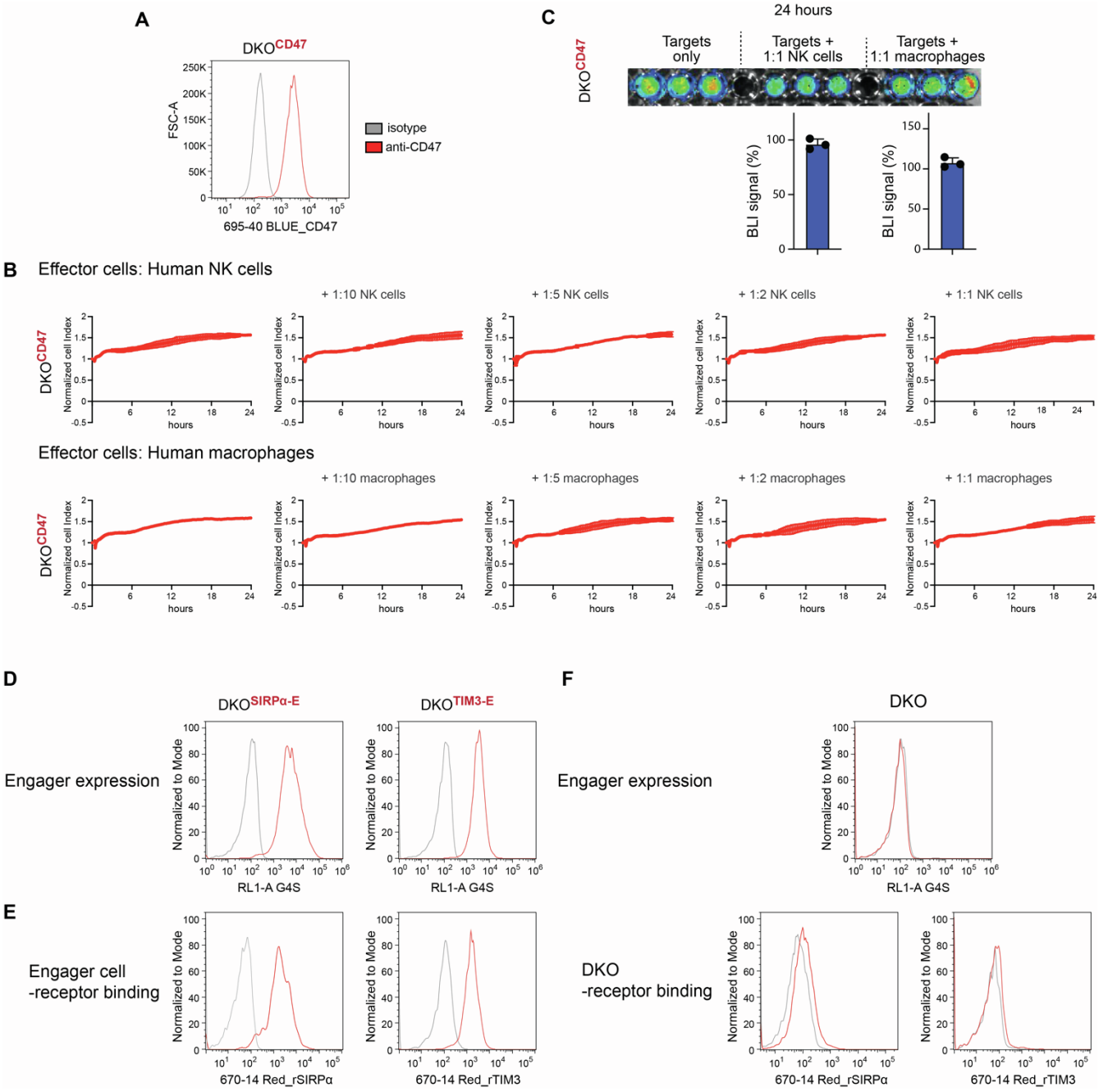

Figure S3: *CD47 reliably protects DKO cells from NK cell and macrophage killing and the SIRPα and TIM3 engagers show good affinity to their respective receptors.* Related to Figure 2.

(A) DKO iECs transduced to express CD47 showed robust CD47 expression.

(B-C) DKO^{CD47} iECs were fully protected against both NK cell and macrophages killing in impedance (B) and BLI (C) assays (mean ± SD per time point, n=3).

(D) The expression of the engager molecules was assessed using a G4S antibody. The engagers for SIRPα and TIM3 were well expressed in the sorted populations (representative flow cytometry histograms).

(E) The binding of the DKO-engager iECs to their respective immune checkpoint receptor was assessed in flow cytometry using recombinant human peptides (rSIRPα and rTIM3, representative flow cytometry histogram). Both engagers showed specific binding.
(F) The binding of DKO iECs not expressing any engager were used as controls and showed minimal binding for rSIRPα and no binding for rTIM3 (representative flow cytometry histograms).

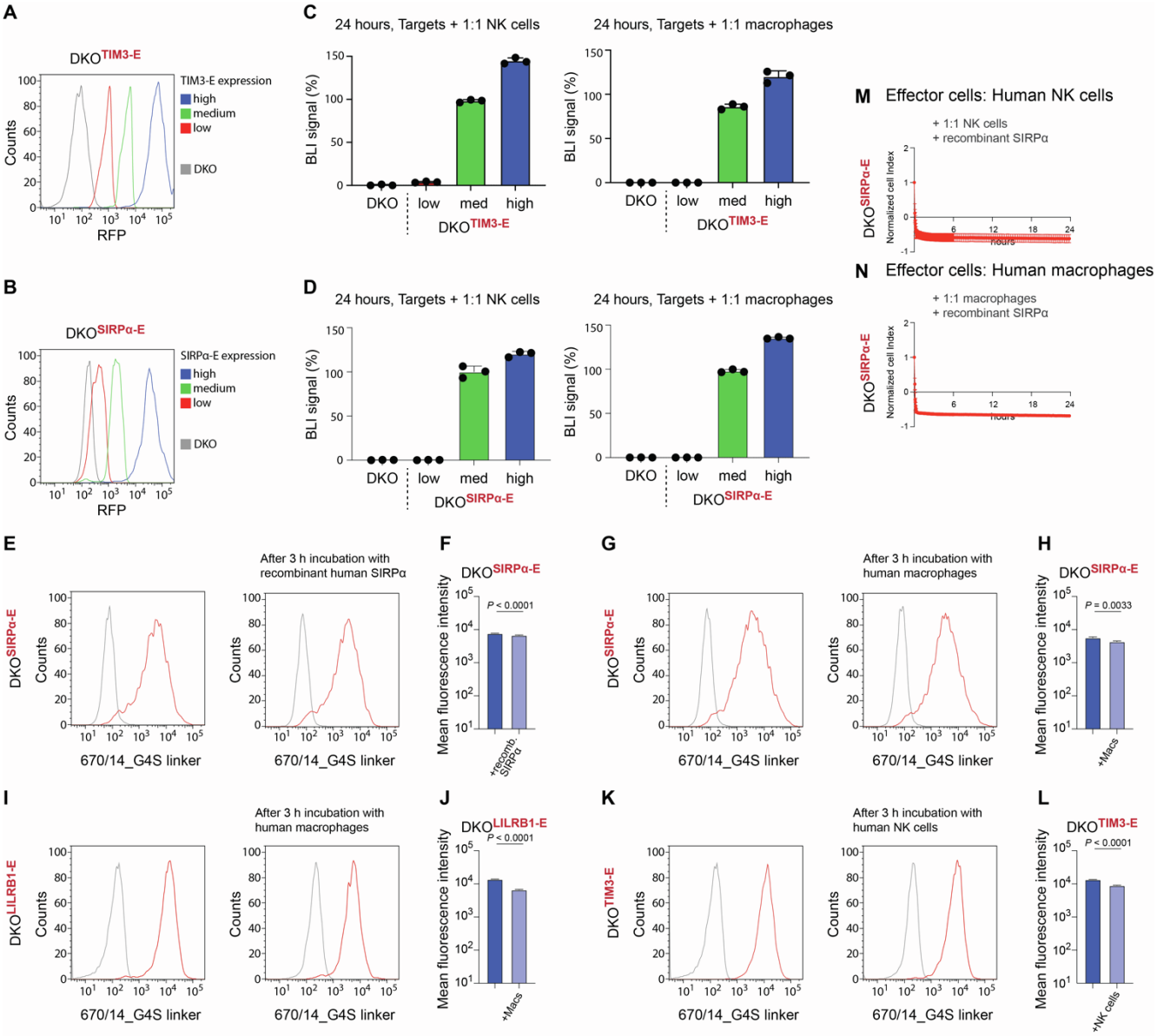

Figure S4: *Correlation of engager expression with inhibitory function and expression dynamics upon receptor binding.* Related to Figure 2.

(A-B) iECs were transduced with lentiviruses for the TIM3 (A) or SIRPα engager (B) and populations with low, medium, and high expression were sorted and directly used in BLI killing assays.

(C-D) BLI killing assays with the sorted iEC populations and NK cells or macrophages as effector cells were performed (mean ± SD, n=3).

(E-H) The surface expression of the SIRPα engager on DKO$^{SIRPα-E}$ iECs was assessed before and 3 hours after incubation with human rSIRPα (E) or macrophages (G, representative flow cytometry histograms). Ligation of the SIRPα engager reduced its surface expression (mean ± SD, n=3, F, H).

(I-J) The surface expression of the LILRB1 engager on DKO$^{LILRB1-E}$ iECs was assessed before and 3 hours after incubation with macrophages (representative flow cytometry histograms, I). Ligation of the LILRB1 engager reduced its surface expression (mean ± SD, n=3, J).

(K-L) The surface expression of the TIM3 engager on DKO$^{TIM3\text{-}E}$ iECs was assessed before and 3 hours after incubation with NK cells (representative flow cytometry histograms, K). Ligation of the TIM3 engager reduced its surface expression (mean ± SD, n=3, L).
(M-N) DKO$^{SIRP\alpha\text{-}E}$ iECs were challenged with NK cells (M) or macrophages (N) in impedance cytotoxicity assays in the presence of 1 μg/ml rSIRPα in an attempt to saturate the engager (mean ± SD per time point, n=3).

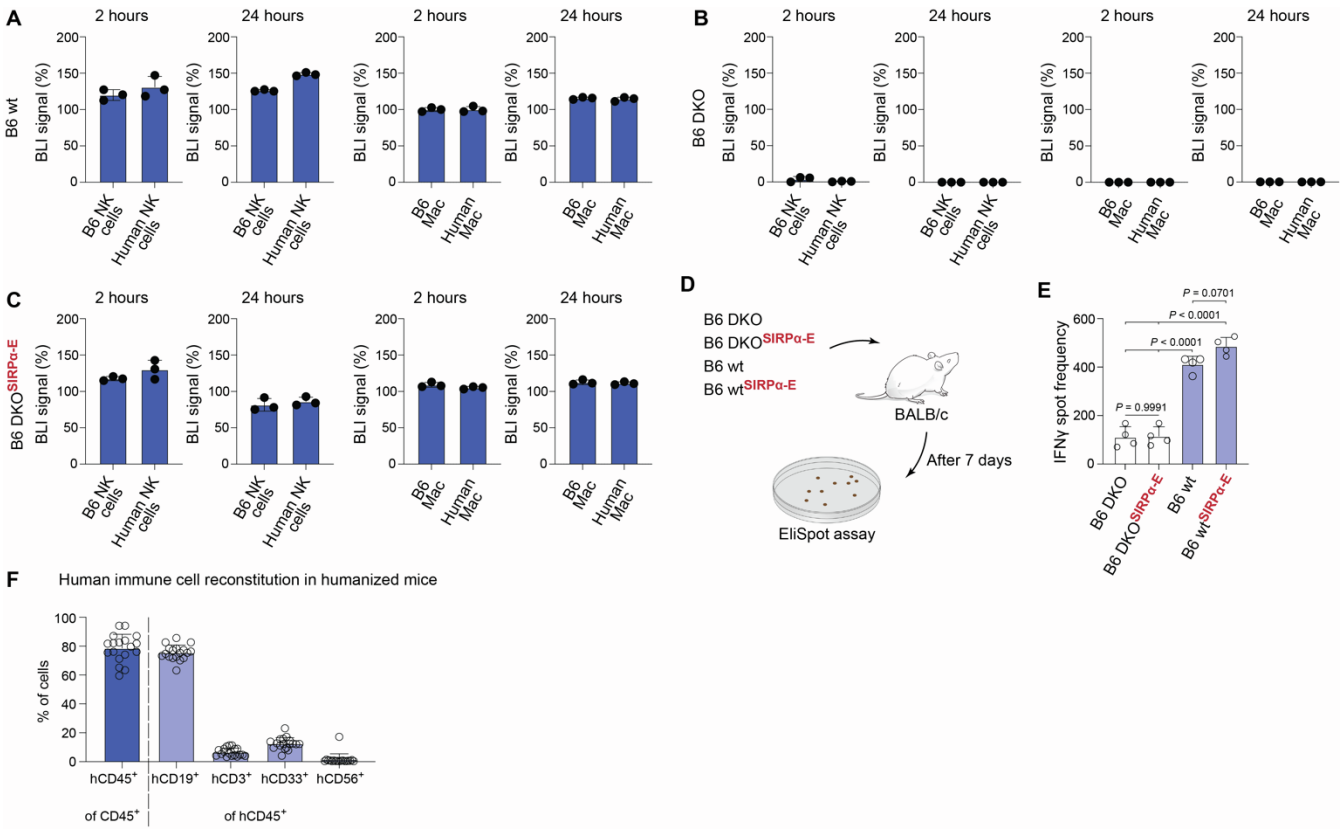

Figure S5: *The SIRPα engager also protects DKO cells from mouse NK cells and macrophages.* Related to Figure 2.

(A-C) B6 wt (A), DKO (B), and DKO$^{SIRP\alpha\text{-}E}$ cells (C) were challenged with human and mouse NK cells and macrophages in BLI killing assays (mean ± SD, n=3).

(D-E) B6 DKO, DKO$^{SIRP\alpha\text{-}E}$, wt, and wt$^{SIRP\alpha\text{-}E}$ cells were injected into allogeneic BALB/c mice (D). After 7 days, splenocytes were recovered for in vitro ELISpot assays (E). ELISpot frequencies were quantified and compared between groups (mean ± SD, n=4).

(F) The reconstitution of human CD45^{+} cells among all CD45+ cells in the humanized mice was assessed, and further the human immune cell subpopulations among the human cells were quantified (mean ± SD, n=18).

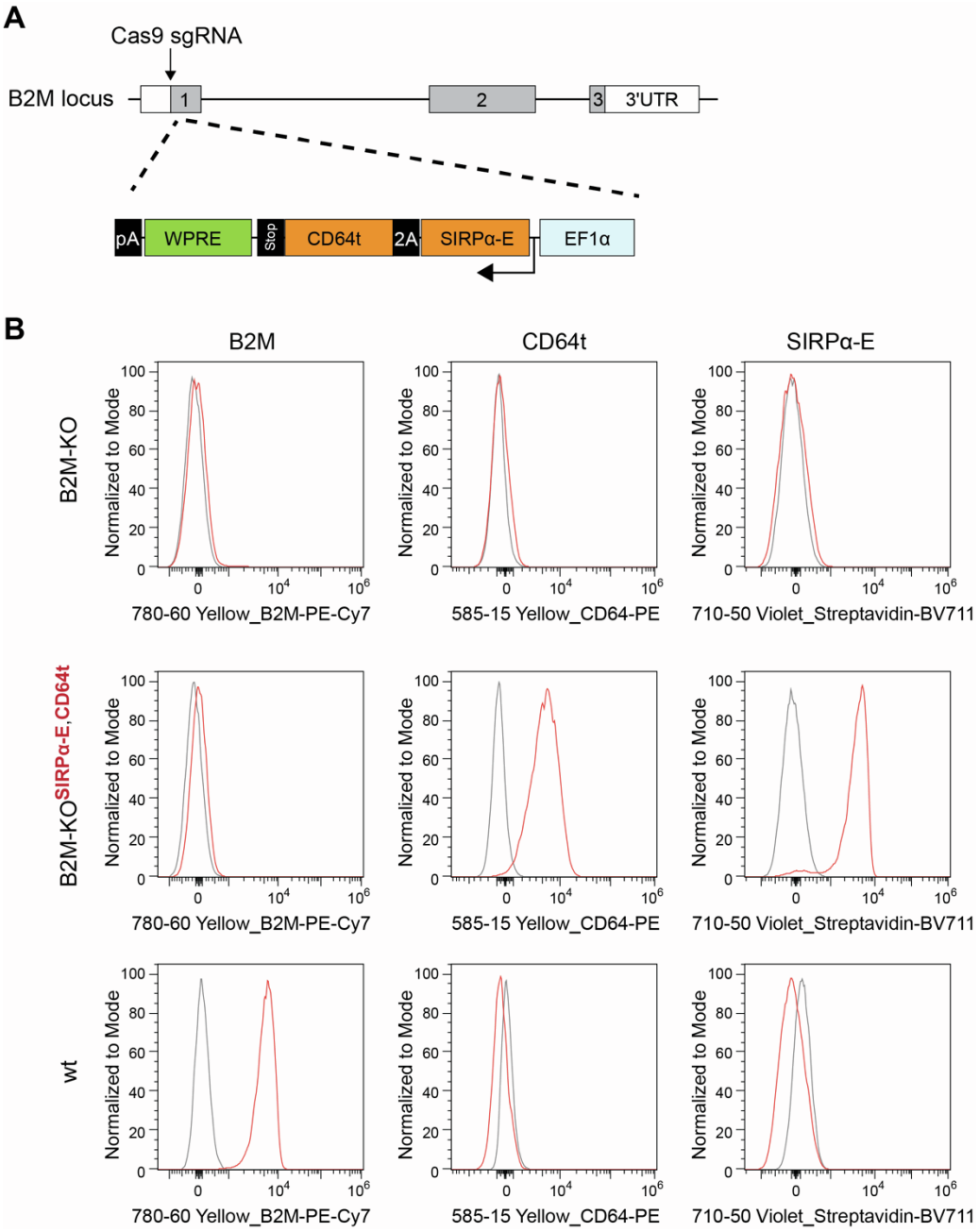

Figure S6: *Non-viral knock-in of SIRPα engager and CD64t into the B2M locus in iPSCs.* Related to Figure 3.

(A) The donor template for Cas9 editing was designed to create a bicistronic transcript of CD64t and the SIRPα engager.

(B) The expression of B2M, CD64t, and SIRPα-E in B2M-KO, B2M-KO$^{CD64t,SIRP\alpha\text{-}E}$, and wt Ff-I01s04 iPSCs is shown (representative flow cytometry histograms).

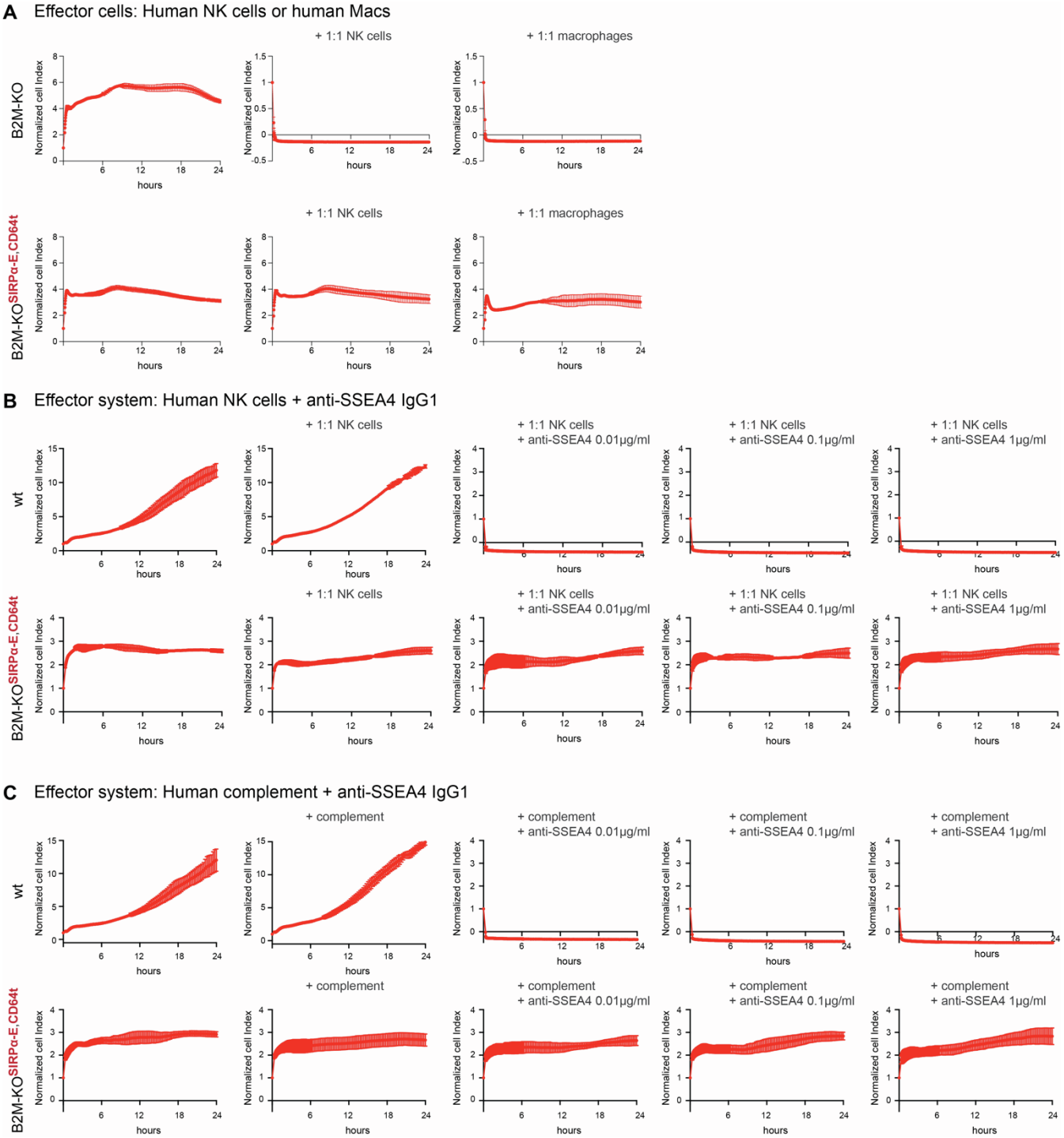

Figure S7: *Non-viral knock-in of SIRPα engager and CD64t protect B2M knockout iPSCs from innate immune cells, ADCC, and CDC.* Related Figure 3.

(A) B2M-KO iPSCs were killed by both NK cells and macrophages, while B2M-KO$^{SIRP\alpha\text{-}E,CD64t}$ iPSCs were protected (mean ± SD per time point, n=3).

(B) wt iPSCs were killed in NK cell ADCC assays using the cytotoxic anti-SSEA-4 IgG1 antibody across a wide range of concentrations, while B2M-KO$^{SIRP\alpha\text{-}E,CD64t}$ iPSCs resisted antibody-mediated cytotoxicity (mean ± SD per time point, n=3).

(C) wt iPSCs were killed in CDC assays using the cytotoxic anti-SSEA-4 IgG1 antibody across a wide range of concentrations, while B2M-KO$^{SIRP\alpha\text{-}E,CD64t}$ iPSCs resisted complement-mediated killing (mean ± SD per time point, n=3).